
How Powerful are K -hop Message Passing Graph Neural Networks

Jiarui Feng^{1,2} Yixin Chen¹ Fuhai Li² Anindya Sarkar¹ Muhan Zhang^{3,4}

{feng.jiarui, fuhai.li, anindya}@wustl.edu,
chen@cse.wustl.edu, muhan@pku.edu.cn

¹Department of CSE, Washington University in St. Louis

²Institute for Informatics, Washington University School of Medicine

³Institute for Artificial Intelligence, Peking University

⁴Beijing Institute for General Artificial Intelligence

Abstract

The most popular design paradigm for Graph Neural Networks (GNNs) is 1-hop message passing—aggregating features from 1-hop neighbors repeatedly. However, the expressive power of 1-hop message passing is bounded by the Weisfeiler-Lehman (1-WL) test. Recently, researchers extended 1-hop message passing to K -hop message passing by aggregating information from K -hop neighbors of nodes simultaneously. However, there is no work on analyzing the expressive power of K -hop message passing. In this work, we theoretically characterize the expressive power of K -hop message passing. Specifically, we first formally differentiate two kinds of kernels of K -hop message passing which are often misused in previous works. We then characterize the expressive power of K -hop message passing by showing that it is more powerful than 1-hop message passing. Despite the higher expressive power, we show that K -hop message passing still cannot distinguish some simple regular graphs. To further enhance its expressive power, we introduce a KP-GNN framework, which improves K -hop message passing by leveraging the peripheral subgraph information in each hop. We prove that KP-GNN can distinguish almost all regular graphs including some distance regular graphs which could not be distinguished by previous distance encoding methods. Experimental results verify the expressive power and effectiveness of KP-GNN. KP-GNN achieves competitive results across all benchmark datasets.

1 Introduction

Currently, most existing graph neural networks (GNNs) follow the *message passing* framework, which iteratively aggregates information from the neighbors and updates the representations of nodes. It has shown superior performance on graph-related tasks [1, 2, 3, 4, 5, 6, 7] comparing to traditional graph embedding techniques [8, 9]. However, as the procedure of message passing is similar to the 1-dimensional Weisfeiler-Lehman (1-WL) test [10], the expressive power of message passing GNNs is also bounded by the 1-WL test [7]. Namely, GNNs cannot distinguish two non-isomorphic graph structures if the 1-WL test would fail.

In normal message passing GNNs, the node representation is updated by the direct neighbors of the node, which are called 1-hop neighbors. Recently, some works extend the notion of message passing into K -hop message passing [11, 12, 13, 14, 15]. **K -hop message passing** is a type of message passing where the node representation is updated by aggregating information from not only 1-hop, but all the neighbors within K hops of the node. However, there is no work on theoretically characterizing the expressive power of GNNs with K -hop message passing, e.g., whether it can improve the 1-hop message passing or not, and to what extent it can.

In this work, we theoretically characterize the expressive power of K -hop message passing GNNs. Specifically, 1) we formally distinguish two different kernels of the K -hop neighbors, which are often misused in previous works. The first kernel is based on whether the node can be reached within k steps of graph diffusion process, which is used in GPR-GNN [14] and MixHop [11]. The second one is based on the shortest path distance of k , which is used in GINE+ [15]. Further, we show that different kernels of K -hop neighbors will result in **different expressive power** of K -hop message passing. 2) We theoretically characterize the expressive power of K -hop message passing GNNs and generalize the proposed theorem to most existing K -hop models. 3) We show that **K -hop message passing is strictly more powerful than 1-hop message passing but bounded by 3-WL** and it failed in distinguishing some simple regular graphs, no matter which kernel is used. This motivates us to further improve K -hop message passing.

Specifically, we introduce **KP-GNN**, a new GNN framework with K -hop message passing, which significantly improves the expressive power of standard K -hop message passing GNNs. In particular, during the aggregation of neighbors in each hop, KP-GNN not only aggregates neighboring nodes in that hop but also aggregates the **peripheral subgraph** (subgraph induced by the neighbors in that hop). This additional information helps the GNN to learn more expressive local structural features around the node. We further prove that KP-GNN is able to distinguish almost all regular graphs and even some distance regular graphs. The proposed KP-GNN has several additional advantages. First, it can be applied to most existing message passing GNNs with little modification. Second, it adds little computational complexity to standard K -hop message passing. We demonstrate the effectiveness of the KP-GNN framework through extensive experiments on both classification and regression tasks.

2 K -hop message passing and its representation power

2.1 Notations

Denote a graph as $G = (V, E)$, where $V = \{1, 2, \dots, n\}$ is the node set and $E \subseteq V \times V$ is the edge set. Meanwhile, denote $A \in \{0, 1\}^{n \times n}$ as the adjacency matrix of graph G . Denote x_v as the feature vector of node v and denote e_{uv} as the feature vector of the edge from u to v . Finally, we denote $Q_{v,G}^1$ as the set of 1-hop neighbors of node v in graph G and $\mathcal{N}_{v,G}^1 = Q_{v,G}^1 \cup \{v\}$. Note that when we say K -hop neighbors of node v , we mean **all** the neighbors that have distance from node v less than or equal to K . In contrast, k -th hop neighbors mean the neighbors with **exactly** distance k from node v . The definition of distance will be discussed in section 2.3.

2.2 1-hop message passing framework

Currently, most existing GNNs are designed based on 1-hop message passing framework [16]. Denote h_v^l as the output representation of node v at layer l and $h_v^0 = x_v$. Briefly, given a graph G and a 1-hop message passing GNN, at layer l of the GNN, h_v^l is computed by h_v^{l-1} and $\{\{h_u^{l-1} \mid u \in Q_{v,G}^1\}\}$:

$$m_v^l = \text{MES}^l(\{\{h_u^{l-1}, e_{uv}\} \mid u \in Q_{v,G}^1\}), \quad h_v^l = \text{UPD}^l(m_v^l, h_v^{l-1}), \quad (1)$$

where m_v^l is the message to node v at layer l , MES^l and UPD^l are message and update functions at layer l respectively. After L layers of message passing, h_v^L is used as the final node representation of node v . Such a representation can be used to conduct node-level tasks like node classification and node regression. To get the graph representation, a readout function is used:

$$h_G = \text{READOUT}(\{\{h_v^L \mid v \in V\}\}), \quad (2)$$

where READOUT is the readout function for computing the final graph representation. Then h_G can be used to conduct graph-level tasks like graph classification and graph regression.

2.3 K -hop message passing framework

The 1-hop message passing framework can be directly generalized to K -hop message passing, as it shares the same message and update mechanism. The difference is that an independent message and update function can be employed for each hop. Meanwhile, a combination function is needed to combine the results from different hops into the final node representation at this layer. First,

we differentiate two different kernels of K -hop neighbors, which are interchanged and misused in previous research.

The first kernel of K -hop neighbors is *shortest path distance (spd) kernel*. Namely, the k -th hop neighbors of node v in graph G is the set of nodes that have shortest path distance of k from v .

Definition 1. For a node v in graph G , the K -hop neighbors $\mathcal{N}_{v,G}^{K,spd}$ of v based on shortest path distance kernel is the set of nodes that have the shortest path distance from node v **less than or equal to** K . We further denote $Q_{v,G}^{k,spd}$ as the set of nodes in G that are **exactly** the k -th hop neighbors (with shortest path distance of exactly k) and $\mathcal{N}_{v,G}^{0,spd} = Q_{v,G}^{0,spd} = \{v\}$ is the node itself.

The second kernel of the K -hop neighbors is based on *graph diffusion (gd)*.

Definition 2. For a node v in graph G , the K -hop neighbors $\mathcal{N}_{v,G}^{K,gd}$ of v based on graph diffusion kernel is the set of nodes that can diffuse information to node v **within the number of random walk diffusion steps** K with the diffusion kernel A . We further denote $Q_{v,G}^{k,gd}$ as the set of nodes in G that are **exactly** the k -th hop neighbors (nodes that can diffuse information to node v with k diffusion steps) and $\mathcal{N}_{v,G}^{0,gd} = Q_{v,G}^{0,gd} = \{v\}$ is the node itself.

Note that a node can be a k -th hop neighbor of v for multiple k based on the graph diffusion kernel. We include more discussions of K -hop kernels in Appendix A. Next, we formally define the K -hop message passing framework as follows:

$$\begin{aligned} m_v^{l,k} &= \text{MES}_k^l(\{(h_u^{l-1}, e_{uv}) | u \in Q_{v,G}^{k,t}\}), \quad h_v^{l,k} = \text{UPD}_k^l(m_v^{l,k}, h_v^{l-1}), \\ h_v^l &= \text{COMBINE}^l(\{h_v^{l,k} | k = 1, 2, \dots, K\}), \end{aligned} \quad (3)$$

where $t = \{spd, gd\}$ indicates the kernel of K -hop neighbors. Here, for each hop, we can apply unique MES and UPD functions. Note that for $k > 1$, there may not exist the edge feature e_{uv} as edges are not directly connected. But we leave it here since we can use another type of feature to replace it, which is described in Appendix H. Compared to the 1-hop message passing framework described in Equation (1), the COMBINE function is introduced to combine the representations of node v at different hops. **It is easy to see that the L layer 1-WL GNNs are L layer K -hop message passing GNNs with $K = 1$.** We include more discussions of K -hop message passing GNNs in Appendix A. To aid further analysis, we also prove that K -hop message passing can injectively encode the neighbor representations at different hops into h_v^l in Appendix K.

2.4 Expressive power of K -hop message passing framework

In this section, we theoretically analyze the expressive power of K -hop message passing. We assume there is no edge feature and all nodes in the graph have the same feature, which means that GNNs can only distinguish two nodes using the local structure of nodes. Note that including node features only increases the expressive power of GNNs as nodes/graphs are more easily discriminated. It has been proved that the expressive power of 1-hop message passing is bounded by the 1-WL test on discriminating non-isomorphic graphs [7, 17]. In this section, We show that the K -hop message passing is strictly more powerful than 1-WL test when $K > 1$. Across the analysis, we utilize regular graphs as examples to illustrate our theorems since they cannot be distinguished using either 1-hop message passing or the 1-WL test. But our analysis is not limited to regular graphs but is capable of describing any graphs.

To begin the analysis, we first define *proper K -hop message passing GNNs*.

Definition 3. A proper K -hop message passing GNN is a GNN model where the message, update, and combine functions are all injective given the input from a countable space.

A proper K -hop message passing GNN is easy to find due to the universal approximation theorem [18] of neural network and the Deep Set for set operation [19]. In the latter sections, by default all mentioned K -hop message passing GNNs are proper. Next, we introduce node configuration:

Definition 4. The node configuration of node v in graph G within k hops under t kernel is a list $A_{v,G}^{k,t} = (a_{v,G}^{1,t}, a_{v,G}^{2,t}, \dots, a_{v,G}^{k,t})$, where $a_{v,G}^{i,t} = |Q_{v,G}^{i,t}|$ is the number of i -th hop neighbors of node v .

When we say two node configurations $A_{v_1,G^{(1)}}^{k,t}$ and $A_{v_2,G^{(2)}}^{k,t}$ are equal, we mean that these two lists are component-wise equal to each other. Now, we state the first proposition:

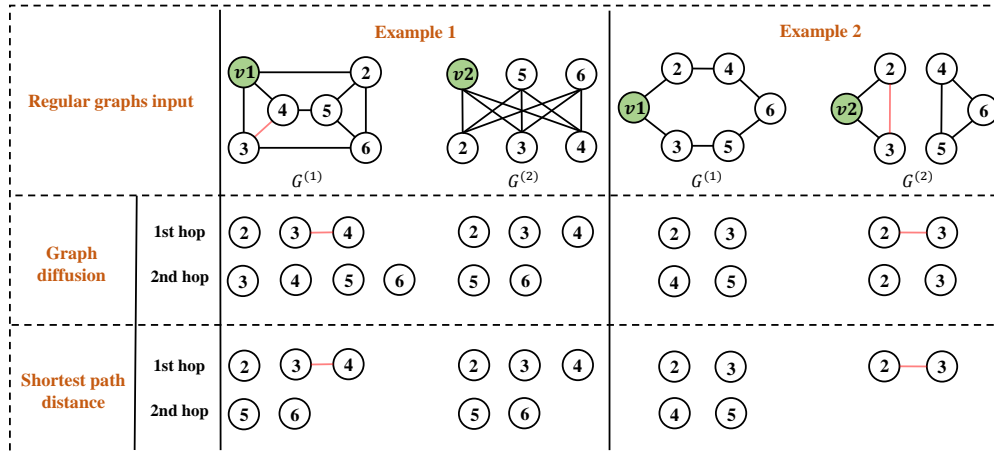


Figure 1: Here are two pairs of non-isomorphic regular graphs. With 2-hop message passing, example 1 can be distinguished by graph diffusion kernel and example 2 can be distinguished by shortest path distance kernel. However, it is indistinguishable if we switch the kernel. Finally, both two examples can be distinguished by adding peripheral edge information.

Proposition 1. *A proper K -hop message passing GNN is strictly more powerful than 1-hop message passing GNNs when $K > 1$.*

To see why this is true, we first discuss how node configuration is related to the first layer of message passing. In the first layer of K -hop message passing, each node aggregates neighbors from up to K hops. As each node has identical label, an injective message function can only know how many neighbors at each hop, which is exactly the node configuration. In other words, **The first layer of K -hop message passing is equivalent to inject node configuration for each node label.** Next, we can characterize the expressive power of 1-hop message passing GNNs using node configuration. When $K = 1$, the node configuration of v_1 and v_2 are $d_{v_1, G^{(1)}}$ and $d_{v_2, G^{(2)}}$, where $d_{v, G}$ is the node degree of v . After L layers, GNNs can get the node degree of each node within L hops of node v . Then, it is straightforward to see why these GNNs cannot distinguish any n -sized r -regular graph, as each node in the regular graph has the same degree. From another perspective, the expressive power of 1-hop message passing GNNs is limited because it only has the degree information of each node in the graph within the receptive field of GNN.

Next, when $K > 1$, the K -hop message passing is at least equally powerful as 1-hop message passing since node configuration up to k hops includes all the information the 1 hop has. To see why it is more powerful, we use two examples to illustrate it. The first example is shown in the left part of Figure 1. Suppose here we use graph diffusion kernel and we want to learn the representation of node v_1 and node v_2 in the two graphs, we know that the 1-hop message passing framework produces the same representation for two nodes as they are both nodes in 6-sized 3-regular graphs. However, it is easy to see that v_1 and v_2 have different local structures and should have different representations. Instead, if we use the 2-hop message passing with the graph diffusion kernel, we can easily distinguish two nodes by checking the 2nd hop neighbors of the node, as node v_1 has four 2nd hop neighbors but node v_2 only has two 2nd hop neighbors. The second example is shown in the right part of Figure 1. Two graphs in the example are still regular graphs and the 1-hop message passing GNNs continue to fail in distinguishing node v_1 and node v_2 . In contrast, suppose here we use shortest path distance kernel, node v_1 and v_2 have different numbers of 2nd hop neighbors and thus will have different representations by performing 2-hop message passing. These two examples convincingly demonstrate that the K -hop message passing with $K > 1$ can have better expressive power than $K = 1$.

The above discussion can be applied to any existing K -hop GNNs using shortest path distance kernel like GINE [15] and Graphormer [20]. However, for K -hop GNNs using graph diffusion kernel like MixHop [11], GPR-GNN [14], and MAGNA [13], we find they actually use a weak version of K -hop than the definition of us. We leave the detailed discussion in Appendix B. Further, Distance Encoding [21] also uses shortest path distance information to augment the 1-hop message passing, which is similar to K -hop GNNs with shortest path distance kernel. However, we find the expressive

power of the two frameworks is actually different from each other. We leave the detailed discussion in Appendix C.

2.5 Limitation of K -hop message passing framework

Although we show that K -hop message passing with $K > 1$ is better at distinguishing non-isomorphic structures than 1-hop message passing, there are still limitations. In this section, we discuss the limitation of K -hop message passing. Specifically, we show that **the choice of the kernel can affect the power of K -hop message passing**. Furthermore, even with K -hop message passing, we **cannot distinguish some simple non-isomorphic structures and the expressive power of K -hop message passing is bounded by 3-WL**.

Continue looking at the provided examples. In example 1, we know that node v_1 and v_2 have different numbers of 2nd hop neighbors with the graph diffusion kernel. However, if we use the shortest path distance kernel, the two nodes have the same number of neighbors in the 2nd hop, which means that we cannot distinguish two nodes using 2-hop message passing with the shortest path distance kernel. Similarly, in example 2, two nodes have the same number of neighbors in both 1st hop and 2nd hops with graph diffusion kernel. These results highlight that the choice of kernel can affect the expressive power of K -hop message passing. Furthermore, **none of them can distinguish both two examples with 2-hop message passing**.

Recently, Frasca et al. [22] show that any subgraph-based GNNs can be implemented by 3-IGN [23, 24] and thus their power is bounded by 3-WL. Here, we show that the K -hop message passing can also be implemented by 3-IGN and thus:

Theorem 1. *The expressive power of a proper K -hop message passing GNN of any kernel is bounded by 3-WL.*

We include the proof in Appendix D. Given all these observations, we may wonder if there is a way to further improve the expressive power of K -hop message passing?

3 KP-GNN: improving the power of K -hop message passing by peripheral subgraph

In this section, we describe how to improve the expressive power of K -hop message passing by adding additional features to message passing. Specifically, by adding the *peripheral subgraph* information, we can improve the representation power of K -hop message passing by a large margin.

3.1 Peripheral edge and peripheral subgraph

First, we define *peripheral edge* and *peripheral subgraph*.

Definition 5. *The peripheral edge $E(Q_{v,G}^{k,t})$ is defined as the set of edges that connect nodes within set $Q_{v,G}^{k,t}$. We further denote $|E(Q_{v,G}^{k,t})|$ as the number of peripheral edge in $E(Q_{v,G}^{k,t})$. The peripheral subgraph $G_{v,G}^{k,t} = (Q_{v,G}^{k,t}, E(Q_{v,G}^{k,t}))$ is defined as the subgraph induced by $Q_{v,G}^{k,t}$ from the whole graph G .*

Briefly speaking, the peripheral edge $E(Q_{v,G}^{k,t})$ record all the edges whose two ends are both from $Q_{v,G}^{k,t}$ and the peripheral subgraph is a graph constituted by peripheral edges. It is easy to see that the peripheral subgraph $G_{v,G}^{k,t}$ automatically contains all the information of peripheral edge $E(Q_{v,G}^{k,t})$. Next, we show that the power of K -hop message passing can be improved by leveraging the information of peripheral edges and peripheral subgraphs. We again refer to the examples in Figure 1. Here we only consider the peripheral edge information. In example 1, we notice that at the 1st hop, there is an edge between node 3 and node 4 in the left graph. More specifically, $E(Q_{v_1,G^{(1)}}^{1,t}) = \{(3, 4)\}$. In contrast, we have $E(Q_{v_2,G^{(2)}}^{1,t}) = \{\}$ in the right graph, which means there is no edge between the 1st hop neighbors of v_2 . Therefore, by adding this information to the message passing, we can successfully distinguish these two nodes. Similarly, in example 2, there is one edge between the 1st hop neighbors of node v_2 but no such edge exists for node v_1 .

By leveraging peripheral edge information, we can distinguish the two nodes as well. The above examples demonstrate the effectiveness of the peripheral edge and peripheral subgraph information.

3.2 K -hop peripheral-subgraph-enhanced graph neural network

In this section, we propose the **K-hop Peripheral-subgraph-enhanced Graph Neural Network (KP-GNN)**, which equips the K -hop message passing with peripheral subgraph information for more powerful GNN design. Recall the K -hop message passing defined in Equation (3). The only difference between KP-GNN is that we revise the message function as follows:

$$\hat{h}_v^{l,k} = \text{MES}_k^l(\{(h_u^{l-1}, e_{uv}) | u \in Q_{v,G}^{k,t}\}, G_{v,G}^{k,t}). \quad (4)$$

Briefly speaking, in the message step at the k -th hop, we not only aggregate information of the neighbors but also the peripheral subgraph at the k -th hop. The implementation of KP-GNN can be very flexible as any graph encoding function can be used. To maximize the information the model can encode while keeping it simple, we implement the message function as:

$$\text{MES}_k^l = \text{MES}_k^{l,normal}(\{(h_u^{l-1}, e_{uv}) | u \in Q_{v,G}^{k,t}\}) + \sum_{c \in C} \frac{1}{|C|} \sum_{(i,j) \in E(Q_{v,G}^{k,t})_c} e_{ij}, \quad (5)$$

where $\text{MES}_k^{l,normal}$ denotes the message function in the original GNN model, C is the set of connected components in $G_{v,G}^{k,t}$, $E(Q_{v,G}^{k,t})_c$ is the edge set of the c -th connected component in $G_{v,G}^{k,t}$. Such implementation helps the KP-GNN to not only encode the $E(Q_{v,G}^{k,t})$ but also partial information of $G_{v,G}^{k,t}$ (number of components). With this implementation, any GNN model can be incorporated into and be enhanced by the KP-GNN framework by replacing $\text{MES}_k^{l,normal}$ and UPD_k^l with the corresponding functions for each hop k . We leave the detailed implementation in Appendix H.

3.3 The expressive power of KP-GNN

In this section, we theoretically characterize the expressive power of KP-GNN and compare it with the original K -hop message passing framework. The key insight is that, according to Equation (4), the message function at the k -th hop additionally encodes $G_{v,G}^{k,t}$ compared to normal K -hop message passing. Next, we show that even with very simple information, the KP-GNN can become powerful enough for distinguishing regular graphs.

Theorem 2. *Consider all pairs of n -sized r -regular graphs, where $3 \leq r < \sqrt{2 \log n}$. For any small constant $\epsilon > 0$, there exists a KP-GNN using shortest path distance as kernel and only peripheral edge information with at most $K = \lceil (\frac{1}{2} + \epsilon \frac{\log n}{\log(r-1-\epsilon)}) \rceil$, which distinguishes almost all $(1 - o(1))$ such pair of graphs with only 1-layer message passing.*

We include the proof in Appendix E. The above theorem proves that a simple implementation of KP-GNN leveraging only peripheral edge information can distinguish almost all regular graphs with some K and 1 layer.

Moreover, K -hop message passing with the shortest path distance kernel cannot distinguish any distance regular graphs with the same intersection array according to the Theorem 3.7 in Distance Encoding [21]. Here we show that KP-GNN is more powerful than Distance Encoding on **distinguishing distance regular graphs**.

Theorem 3. *For two non-isomorphic distance regular graphs $G^{(1)} = (V^{(1)}, E^{(1)})$ and $G^{(2)} = (V^{(2)}, E^{(2)})$ with the same intersection array $(b_0, b_1, \dots, b_{d-1}; c_1, c_2, \dots, c_d)$, we pick two nodes v_1 and v_2 from two graphs respectively. Given a proper 1-layer K -hop KP-GNN with message functions defined in Equation (5), it can distinguish v_1 and v_2 if $b_0 - b_j - c_j = 2$ for some $j \leq K$ and $G_{v_1,G^{(1)}}^{j,t}$ and $G_{v_2,G^{(2)}}^{j,t}$ are non-isomorphic.*

We include the proof in Appendix F. Theorem 3 shows that the KP-GNN with a simple implementation can distinguish some distance regular graphs, which further distinguishes KP-GNN from Distance Encoding [21] and subgraph-based GNNs [25, 26, 27, 28] as they cannot distinguish distance regular graphs. We include further discussion in Appendix F. However, with the current implementation, KP-GNN cannot distinguish all distance regular graphs.

3.4 Time, space complexity, and limitation

In this section, we discuss the time and space complexity of K -hop message passing GNN and KP-GNN. Suppose a graph has n nodes and m edges. Then, the K -hop message passing and KP-GNN have both the space complexity of $O(n)$ and time complexity of $O(n^2)$ for the shortest path distance kernel. Note that the complexity of graph diffusion is no less than the shortest path distance kernel. We can see that KP-GNN only requires the same space complexity as vanilla GNNs and much less time complexity than the $O(nm)$ of subgraph-based GNNs. We leave the detailed discussion on the complexity and limitation of KP-GNN in Appendix G.

4 Related Work

Expressive power of GNN. Analyzing the expressive power of GNNs is a crucial problem as it can serve as a guide on how to improve GNNs. Xu et al. [7] and Morris et al. [17] first proved that the power of 1-hop message passing is bounded by the 1-WL test. In other words, 1-hop message passing cannot distinguish any non-isomorphic graphs that the 1-WL test fails to. In recent years, many efforts have been put into increasing the expressive power of 1-hop messaging passing. The first line of research tries to mimic the higher-order WL tests, like 1-2-3 GNN [17], PPGN [23], ring-GNN [29]. However, they require exponentially increasing space and time complexity w.r.t. node number and cannot be generalized to large-scale graphs. The second line of research tries to enhance the rooted subtree of 1-WL with additional features. Some works [30, 31, 32] add one-hot or random features into nodes. Although they achieve good results in some settings, they deteriorate the generalization ability as such features produce different representations for nodes even with the same local graph structure. Some works like Distance Encoding [21], SEAL [33], labeling trick [34] and GLASS [35] introduce node labeling based on either distance or distinguishing target node set. On the other hand, GraphSNN [36] introduces a hierarchy of local isomorphism and proposes structural coefficients as additional features to identify such local isomorphism. However, the function designed to approximate the structural coefficient cannot fully achieve its theoretical power. The third line of research resorts to subgraph representation. Specifically, ID-GNN [37] extracts ego-network for each node and label the root node with a different color. NGNN [25] encodes a rooted subgraph instead of a rooted subtree by subgraph pooling thus achieving superior expressive power on distinguishing regular graphs. GNN-AK [26] applies a similar idea as NGNN. The only difference lies in how to compute the node representation from the local subgraph. However, such methods need to run an inner GNN on every node of the graph thus introducing much more computation overhead. Meanwhile, the expressive power of subgraph GNNs are bounded by 3-WL [22].

K -hop message passing GNN. There are some existing works that instantiate the K -hop message passing framework. For example, MixHop [11] performs message passing on each hop with graph diffusion kernel and concatenates the representation on each hop as the final representation. K-hop [12] sequentially performs the message passing from hop K to hop 1 to compute the representation of the center node. However, it is not parallelizable due to its computational procedure. MAGNA [13] introduces an attention mechanism to K -hop message passing. GPR-GNN [14] use graph diffusion kernel to perform graph convolution on K -hop and aggregate them with learnable parameters. However, none of them give a formal definition of K -hop message passing and theoretically analyze its representation power and limitations.

5 Experiments

In this section, we conduct extensive experiments to evaluate the performance of KP-GNN. Specifically, we 1) empirically verify the expressive power of KP-GNN on 3 simulation datasets and demonstrate the benefits of KP-GNN compared to normal K -hop message passing GNNs and existing models; 2) show that the KP-GNN can achieve state-of-the-art performance on 5 TU datasets; 3) demonstrate that the KP-GNN achieves comparable performance on 3 molecular prediction datasets; 4) analyze the running time of KP-GNN. The detail of each variant of KP-GNN is described in Appendix H and the detailed experimental setting is described in Appendix I.

Datasets: To evaluate the expressive power of KP-GNN, we choose: 1) EXP dataset [38], which contains 600 pairs of 1-WL-indistinguishable but non-isomorphic graphs. 2) Graph property regression (connectedness, diameter, radius) and node property regression (single source shortest path, eccentric-

Table 1: Simulation dataset result. The top two are highlighted by **First**, **Second** . (*: with encoding)

Method	EXP(ACC)	Node Properties ($\log_{10}(\text{MAE})$)			Graph Properties ($\log_{10}(\text{MAE})$)			Counting Substructures (MAE)			
		SSSP	Ecc.	Lap.	Connect.	Diameter	Radius	Tri.	Tailed Tri.	Star	4-Cycle
GIN	50	-2.0000	-1.9000	-1.6000	-1.9239	-3.3079	-4.7584	0.3569	0.2373	0.0224	0.2185
PNA	50	-2.8900	-2.8900	-3.7700	-1.9395	3.4382	-4.9470	0.3532	0.2648	0.1278	0.2430
PPGN	100	-	-	-	-1.9804	-3.6147	-5.0878	0.0089	0.0096	0.0148	0.0090
GIN-AK+	100	-	-	-	-2.2268	-3.7585	-5.1044	0.0885	0.0696	0.0162	0.0668
K-GIN+	100	-2.7651	-2.6159	-4.4309	-2.0725	-3.9732	-5.3113	0.1180	0.0747	0.0009	0.0840
KP-GIN+	100	-2.7651	-2.6193	-4.6107	-4.1803	-3.9952	-5.2206	0.0377	0.0314	0.0024	0.0258
GIN-AK+*	100	-	-	-	-2.7513	-3.9687	5.1846	0.0123	0.0112	0.0150	0.0126
KP-GIN+*	100	-2.7628	-2.6164	-4.3540	-3.7229	-4.0160	-5.2357	0.0029	0.0027	0.0029	0.0082

ity, Laplacian feature) task on graph random dataset [39]. 3) Graph substructure counting (triangle, tailed triangle, star and 4-cycle) tasks on random graph dataset [40]. For TU datasets evaluation, we choose MUTAG [41], D&D [42], PROTEINS [42], PTC-MR [43], and IMDB-B [44] from TU database. For molecule prediction datasets, we pick QM9 [45, 46], ZINC [47], and MolHIV [48]. The detailed statistics of the datasets are described in Appendix J. Without further highlight, all error bars in the result tables are standard deviation of multiple runs (more details are in Appendix I).

Table 2: Ablation study on EXP

kernel	K	K-GIN+	KP-GIN+
GD	$K=1$	50	50
	$K=2$	50	100
	$K=3$	66.17	100
	$K=4$	100	100
SPD	$K=1$	50	50
	$K=2$	50	100
	$K=3$	100	100
	$K=4$	100	100

Empirical verification of the expressive power: To evaluate the power of KP-GNN, we compare it with several existing models. For the baseline model, we use GIN [7], which has the same expressive power as 1-WL test. For more powerful baselines, we use GIN-AK+ [26], PNA [39] and PPGN [23]. For KP-GNN, we implement the KP-GIN+. To evaluate the effectiveness of the peripheral subgraph, we also implement the normal K -hop version of GINE+, denote as K-GIN+. The results are

shown in Table 1. Baseline results are taken from [26] and [39]. We also compare results of GIN-AK+ for both with and without D2C encoding and KP-GIN+ both with and without path encoding. We can see both K-GIN+ and KP-GIN+ achieve perfect performance on EXP dataset. Further, we conduct an ablation study on KP-GIN+ and K-GIN+ using EXP dataset. Table 2 presents the results. We can see that KP-GNN achieves perfect results with only $K \geq 2$ for both two kernels. However, K-GIN requires $K \geq 3$ and $K \geq 4$ to get perfect results for shortest path distance kernel and graph diffusion kernel respectively. Results on various property regression tasks further demonstrate the advantage of KP-GNN over existing models and normal K -hop message passing GNNs.

Table 3: TU dataset evaluation result.

Method	MUTAG	D&D	PTC-MR	PROTEINS	IMDB-B
WL	90.4±5.7	79.4±0.3	59.9±4.3	75.0±3.1	73.8±3.9
GIN	89.4±5.6	-	64.6±7.0	75.9±2.8	75.1±5.1
DGCNN	85.8±1.7	79.3 ±0.9	58.6 ±2.5	75.5±0.9	70.0±0.9
GraphSNN	91.24±2.5	82.46 ±2.7	66.96±3.5	76.51 ±2.5	76.93±3.3
GIN-AK+	91.30±7.0	-	68.20±5.6	77.10±5.7	75.60±3.7
KP-GCN	91.1±6.0	78.9±3.9	64.1±7.9	76.4±4.8	75.1±3.6
KP-GraphSAGE	91.1±3.9	78.2±3.7	65.9±7.6	76.1±4.4	74.7±3.7
KP-GIN	91.1±5.4	78.6±4.3	64.7±6.8	76.1±5.4	74.4±3.4
GIN-AK+*	95.0±6.1	OOM	74.1±5.9	78.9±5.4	77.3±3.1
GraphSNN*	94.70±1.9	83.93±2.3	70.58±3.1	78.42±2.7	78.51±2.8
KP-GCN*	96.1±4.6	83.1±2.8	72.4±5.8	80.0±3.8	79.0±2.7
KP-GraphSAGE*	96.1±4.6	84.0±3.4	74.4±6.5	79.9±4.2	78.7±4.0
KP-GIN*	95.6±5.1	82.9±2.3	71.8±6.8	79.8±3.8	78.0±3.7

Evaluation on TU datasets: For baseline models, we select: 1) graph kernel based method WL subtree kernel [49]; 2) 1-hop message passing based GNN methods: GIN [7] and DGCNN [6]; 3) advanced GNN methods: GraphSNN [36] and GIN-AK+ [26]. For the proposed KP-GNN, we implement GCN [1], GraphSAGE [3], and GIN [7] using the KP-GNN framework, denoted as KP-GCN, KP-GraphSAGE, and KP-GIN respectively. The results are shown in Table 3. For a detailed comparison, we report the results of two different settings. The first setting follows Xu et al. [7] and the second setting follows Wijesinghe and Wang [36]. We denote the second setting with * in the table.

Table 4: QM9 results. The top two are highlighted by **First**, **Second**

Target	DTNN	MPNN	Deep LRP	PPGN	Nested 1-2-3-GNN	KP-GIN+
μ	0.244	0.358	0.364	0.231	0.433	0.365
α	0.95	0.89	0.298	0.382	0.265	0.249
$\varepsilon_{\text{HOMO}}$	0.00388	0.00541	0.00254	0.00276	0.00279	0.00243
$\varepsilon_{\text{LUMO}}$	0.00512	0.00623	0.00277	0.00287	0.00276	0.00252
$\Delta\varepsilon$	0.0112	0.0066	0.00353	0.00406	0.00390	0.00346
$\langle R^2 \rangle$	17.0	28.5	19.3	16.7	20.1	16.64
ZPVE	0.00172	0.00216	0.00055	0.00064	0.00015	0.00017
U_0	2.43	2.05	0.413	0.234	0.205	0.06632
U	2.43	2.00	0.413	0.234	0.200	0.09447
H	2.43	2.02	0.413	0.229	0.249	0.06037
G	2.43	2.02	0.413	0.238	0.253	0.04752
C_v	0.27	0.42	0.129	0.184	0.0811	0.0977

We can see that under the setting of Wijesinghe and Wang [36], KP-GNN achieves state-of-the-art performance across all datasets, which demonstrates the performance of KP-GNN on real-world datasets. Under the setting of Xu et al. [7], KP-GNN still achieves comparable performance.

Evaluation on molecular prediction tasks: For QM9 dataset, we report results of DTNN and MPNN from [46]. We further select Deep LRP [40], PPGN [23], and Nested 1-2-3-GNN [25] as baseline models. For ZINC dataset, we report results of MPNN [16] and PNA [39] from [47]. We further pick Graphormer [20], GSN [50], GIN-AK+ [26], and CIN [51]. For MolHIV dataset, we report results of PNA [39], DeepLRP [40], GINE [15], NGNN [25], GIN-AK+[26] and GraphSNN [36]. The results of QM9 dataset are shown in Table 4. We can see KP-GNN achieves state-of-the-art performance on most of the targets. The results of MolHIV and ZINC dataset are shown in Table 5 and Table 6. Although KP-GNN does not achieve the best result, it is still comparable to other methods.

Table 5: OGB-MolHIV result.

Method	Test AUC
PNA	79.05 \pm 1.32
DeepLRP	77.19 \pm 1.40
GINE-VN	76.60 \pm 1.40
NGNN	78.34 \pm 1.86
GIN-AK+	79.61 \pm 1.19
GraphSNN-VN	79.72 \pm 1.83
KP-GIN+-VN	78.48 \pm 0.87

Table 6: ZINC result.

Method	# param.	test MAE
MPNN	480805	0.145 \pm 0.007
PNA	387155	0.142 \pm 0.010
Graphormer	489321	0.122 \pm 0.006
GSN	\sim 500000	0.101 \pm 0.010
GIN-AK+	-	0.080 \pm 0.001
CIN	-	0.079 \pm 0.006
KP-GIN+	500790	0.119 \pm 0.002

Table 7: Running time (ms/epoch)

Method	D&D	ZINC	Graph property
GIN	1.15	5.00	1.80
K-GIN	6.55	11.00	3.77
KP-GIN	7.84	13.00	6.82
KP-GIN+	7.96	9.00	8.74

Running time comparison: In this section, we compare the running time of KP-GNN to 1-hop message passing GNN and K -hop message passing GNN. We use GIN [7] as the base model. We also include the KP-GIN+. All models use the same number of layers and hidden dimensions for a fair comparison. The results are shown in Table 7. For D&D, ZINC, and Graph property

dataset, we set $K = 5$, $K = 4$, $K = 6$ respectively. We can see the computational overhead does not seem to grow quadratically as in our theoretical analysis. This is reasonable as practical graphs are sparse and the number of K -hop neighbors is far less than n when using a small K .

6 Conclusion

In this paper, we theoretically characterize the power of K -hop message passing GNNs and propose the KP-GNN to improve the expressive power by leveraging the peripheral subgraph information at each hop. Theoretically, we prove that KP-GNN can distinguish almost all regular graphs including some distance regular graphs. Empirically, KP-GNN achieves competitive results across all simulation and real-world datasets.

References

- [1] Thomas N Kipf and Max Welling. Semi-supervised classification with graph convolutional networks. *arXiv preprint arXiv:1609.02907*, 2016.
- [2] David K Duvenaud, Dougal Maclaurin, Jorge Iparraguirre, Rafael Bombarell, Timothy Hirzel, Alán Aspuru-Guzik, and Ryan P Adams. Convolutional networks on graphs for learning molecular fingerprints. In *Advances in neural information processing systems*, pages 2224–2232, 2015.
- [3] Will Hamilton, Zhitao Ying, and Jure Leskovec. Inductive representation learning on large graphs. In *Advances in Neural Information Processing Systems*, pages 1025–1035, 2017.
- [4] Petar Veličković, Guillem Cucurull, Arantxa Casanova, Adriana Romero, Pietro Lio, and Yoshua Bengio. Graph attention networks. *arXiv preprint arXiv:1710.10903*, 2017.
- [5] Yujia Li, Daniel Tarlow, Marc Brockschmidt, and Richard Zemel. Gated graph sequence neural networks. *arXiv preprint arXiv:1511.05493*, 2015.
- [6] Muhan Zhang, Zhicheng Cui, Marion Neumann, and Yixin Chen. An end-to-end deep learning architecture for graph classification. In *AAAI*, pages 4438–4445, 2018.
- [7] Keyulu Xu, Weihua Hu, Jure Leskovec, and Stefanie Jegelka. How powerful are graph neural networks? *arXiv preprint arXiv:1810.00826*, 2018.
- [8] Aditya Grover and Jure Leskovec. node2vec: Scalable feature learning for networks. In *Proceedings of the 22nd ACM SIGKDD international conference on Knowledge discovery and data mining*, pages 855–864. ACM, 2016.
- [9] Bryan Perozzi, Rami Al-Rfou, and Steven Skiena. Deepwalk: Online learning of social representations. In *Proceedings of the 20th ACM SIGKDD international conference on Knowledge discovery and data mining*, pages 701–710. ACM, 2014.
- [10] Boris Weisfeiler and AA Lehman. A reduction of a graph to a canonical form and an algebra arising during this reduction. *Nauchno-Technicheskaya Informatsia*, 2(9):12–16, 1968.
- [11] Sami Abu-El-Haija, Bryan Perozzi, Amol Kapoor, Nazanin Alipourfard, Kristina Lerman, Hrayr Harutyunyan, Greg Ver Steeg, and Aram Galstyan. Mixhop: Higher-order graph convolutional architectures via sparsified neighborhood mixing. In *international conference on machine learning*, pages 21–29. PMLR, 2019.
- [12] Giannis Nikolentzos, George Dasoulas, and Michalis Vazirgiannis. k-hop graph neural networks. *Neural Networks*, 130:195–205, 2020.
- [13] Guangtao Wang, Zhitao Ying, Jing Huang, and Jure Leskovec. Multi-hop attention graph neural network, 2021. URL <https://openreview.net/forum?id=muppfCkU9H1>.
- [14] Eli Chien, Jianhao Peng, Pan Li, and Olgica Milenkovic. Adaptive universal generalized pagerank graph neural network. In *International Conference on Learning Representations*, 2021. URL <https://openreview.net/forum?id=n6j17fLxrP>.
- [15] Rémy Brossard, Oriel Frigo, and David Dehaene. Graph convolutions that can finally model local structure. *arXiv preprint arXiv:2011.15069*, 2020.
- [16] Justin Gilmer, Samuel S Schoenholz, Patrick F Riley, Oriol Vinyals, and George E Dahl. Neural message passing for quantum chemistry. In *Proceedings of the 34th International Conference on Machine Learning-Volume 70*, pages 1263–1272. JMLR. org, 2017.
- [17] Christopher Morris, Martin Ritzert, Matthias Fey, William L Hamilton, Jan Eric Lenssen, Gaurav Rattan, and Martin Grohe. Weisfeiler and leman go neural: Higher-order graph neural networks. In *Proceedings of the AAAI Conference on Artificial Intelligence*, volume 33, pages 4602–4609, 2019.
- [18] George V. Cybenko. Approximation by superpositions of a sigmoidal function. *Mathematics of Control, Signals and Systems*, 2:303–314, 1989.

- [19] Manzil Zaheer, Satwik Kottur, Siamak Ravanbakhsh, Barnabas Poczos, Russ R Salakhutdinov, and Alexander J Smola. Deep sets. In *Advances in Neural Information Processing Systems*, pages 3391–3401, 2017.
- [20] Chengxuan Ying, Tianle Cai, Shengjie Luo, Shuxin Zheng, Guolin Ke, Di He, Yanming Shen, and Tie-Yan Liu. Do transformers really perform badly for graph representation? In A. Beygelzimer, Y. Dauphin, P. Liang, and J. Wortman Vaughan, editors, *Advances in Neural Information Processing Systems*, 2021. URL <https://openreview.net/forum?id=0eWooOxFwDa>.
- [21] Pan Li, Yanbang Wang, Hongwei Wang, and Jure Leskovec. Distance encoding—design provably more powerful gnns for structural representation learning. *arXiv preprint arXiv:2009.00142*, 2020.
- [22] Fabrizio Frasca, Beatrice Bevilacqua, Michael Bronstein, and Haggai Maron. Understanding and extending subgraph gnns by rethinking their symmetries. *ArXiv*, abs/2206.11140, 2022.
- [23] Haggai Maron, Heli Ben-Hamu, Hadar Serviansky, and Yaron Lipman. Provably powerful graph networks. In *Advances in Neural Information Processing Systems*, pages 2156–2167, 2019.
- [24] Haggai Maron, Heli Ben-Hamu, Nadav Shamir, and Yaron Lipman. Invariant and equivariant graph networks. *arXiv preprint arXiv:1812.09902*, 2018.
- [25] Muhan Zhang and Pan Li. Nested graph neural networks. In A. Beygelzimer, Y. Dauphin, P. Liang, and J. Wortman Vaughan, editors, *Advances in Neural Information Processing Systems*, 2021. URL https://openreview.net/forum?id=7_eLEvFjCi3.
- [26] Lingxiao Zhao, Wei Jin, Leman Akoglu, and Neil Shah. From stars to subgraphs: Uplifting any GNN with local structure awareness. In *International Conference on Learning Representations*, 2022. URL https://openreview.net/forum?id=Mspk_WYKoEH.
- [27] Leonardo Cotta, Christopher Morris, and Bruno Ribeiro. Reconstruction for powerful graph representations. In A. Beygelzimer, Y. Dauphin, P. Liang, and J. Wortman Vaughan, editors, *Advances in Neural Information Processing Systems*, 2021. URL <https://openreview.net/forum?id=ZKbZ4mEbI9L>.
- [28] Beatrice Bevilacqua, Fabrizio Frasca, Derek Lim, Balasubramaniam Srinivasan, Chen Cai, Gopinath Balamurugan, Michael M. Bronstein, and Haggai Maron. Equivariant subgraph aggregation networks. In *International Conference on Learning Representations*, 2022. URL <https://openreview.net/forum?id=dFbKQaRk15w>.
- [29] Zhengdao Chen, Soledad Villar, Lei Chen, and Joan Bruna. On the equivalence between graph isomorphism testing and function approximation with gnns. In *Advances in Neural Information Processing Systems*, pages 15894–15902, 2019.
- [30] Ryoma Sato, Makoto Yamada, and Hisashi Kashima. Random features strengthen graph neural networks. *arXiv preprint arXiv:2002.03155*, 2020.
- [31] Ralph Abboud, Ismail Ilkan Ceylan, Martin Grohe, and Thomas Lukasiewicz. The surprising power of graph neural networks with random node initialization, 2021. URL <https://openreview.net/forum?id=L7Irrt5sMQa>.
- [32] Andreas Loukas. What graph neural networks cannot learn: depth vs width. *arXiv preprint arXiv:1907.03199*, 2019.
- [33] Muhan Zhang and Yixin Chen. Link prediction based on graph neural networks. In *Advances in Neural Information Processing Systems*, pages 5165–5175, 2018.
- [34] Muhan Zhang, Pan Li, Yinglong Xia, Kai Wang, and Long Jin. Labeling trick: A theory of using graph neural networks for multi-node representation learning. In A. Beygelzimer, Y. Dauphin, P. Liang, and J. Wortman Vaughan, editors, *Advances in Neural Information Processing Systems*, 2021. URL <https://openreview.net/forum?id=Hcr9mgBG6ds>.

- [35] Xiyuan Wang and Muhan Zhang. GLASS: GNN with labeling tricks for subgraph representation learning. In *International Conference on Learning Representations*, 2022. URL <https://openreview.net/forum?id=XLxhEjKNbXj>.
- [36] Asiri Wijesinghe and Qing Wang. A new perspective on "how graph neural networks go beyond weisfeiler-lehman?". In *International Conference on Learning Representations*, 2022. URL https://openreview.net/forum?id=uxgg9o7bI_3.
- [37] Jiaxuan You, Jonathan Gomes-Selman, Rex Ying, and Jure Leskovec. Identity-aware graph neural networks. *arXiv preprint arXiv:2101.10320*, 2021.
- [38] Ralph Abboud, İsmail İlkan Ceylan, Martin Grohe, and Thomas Lukasiewicz. The surprising power of graph neural networks with random node initialization. *arXiv preprint arXiv:2010.01179*, 2020.
- [39] Gabriele Corso, Luca Cavalleri, Dominique Beaini, Pietro Liò, and Petar Veličković. Principal neighbourhood aggregation for graph nets. *arXiv preprint arXiv:2004.05718*, 2020.
- [40] Zhengdao Chen, Lei Chen, Soledad Villar, and Joan Bruna. Can graph neural networks count substructures? *Advances in neural information processing systems*, 2020.
- [41] Asim Kumar Debnath, de Compadre RL Lopez, Gargi Debnath, Alan J Shusterman, and Corwin Hansch. Structure-activity relationship of mutagenic aromatic and heteroaromatic nitro compounds. correlation with molecular orbital energies and hydrophobicity. *Journal of medicinal chemistry*, 34(2):786–797, 1991.
- [42] Paul D Dobson and Andrew J Doig. Distinguishing enzyme structures from non-enzymes without alignments. *Journal of molecular biology*, 330(4):771–783, 2003.
- [43] Hannu Toivonen, Ashwin Srinivasan, Ross D King, Stefan Kramer, and Christoph Helma. Statistical evaluation of the predictive toxicology challenge 2000–2001. *Bioinformatics*, 19(10):1183–1193, 2003.
- [44] Pinar Yanardag and SVN Vishwanathan. Deep graph kernels. In *Proceedings of the 21th ACM SIGKDD International Conference on Knowledge Discovery and Data Mining*, pages 1365–1374. ACM, 2015.
- [45] Raghunathan Ramakrishnan, Pavlo O Dral, Matthias Rupp, and O Anatole Von Lilienfeld. Quantum chemistry structures and properties of 134 kilo molecules. *Scientific data*, 1(1):1–7, 2014.
- [46] Zhenqin Wu, Bharath Ramsundar, Evan N Feinberg, Joseph Gomes, Caleb Geniesse, Aneesh S Pappu, Karl Leswing, and Vijay Pande. Moleculenet: a benchmark for molecular machine learning. *Chemical science*, 9(2):513–530, 2018.
- [47] Vijay Prakash Dwivedi, Chaitanya K Joshi, Anh Tuan Luu, Thomas Laurent, Yoshua Bengio, and Xavier Bresson. Benchmarking graph neural networks. *arXiv preprint arXiv:2003.00982*, 2020.
- [48] Weihua Hu, Matthias Fey, Marinka Zitnik, Yuxiao Dong, Hongyu Ren, Bowen Liu, Michele Catasta, and Jure Leskovec. Open graph benchmark: Datasets for machine learning on graphs. *arXiv preprint arXiv:2005.00687*, 2020.
- [49] Nino Shervashidze, Pascal Schweitzer, Erik Jan van Leeuwen, Kurt Mehlhorn, and Karsten M Borgwardt. Weisfeiler-lehman graph kernels. *Journal of Machine Learning Research*, 12(Sep):2539–2561, 2011.
- [50] Giorgos Bouritsas, Fabrizio Frasca, Stefanos Zafeiriou, and Michael M. Bronstein. Improving graph neural network expressivity via subgraph isomorphism counting, 2021. URL <https://openreview.net/forum?id=LTOKSFnQDWF>.
- [51] Cristian Bodnar, Fabrizio Frasca, Nina Otter, Yu Guang Wang, Pietro Liò, Guido Montufar, and Michael M. Bronstein. Weisfeiler and lehman go cellular: CW networks. In A. Beygelzimer, Y. Dauphin, P. Liang, and J. Wortman Vaughan, editors, *Advances in Neural Information Processing Systems*, 2021. URL <https://openreview.net/forum?id=uVPZCMVtsSG>.

- [52] Ashish Vaswani, Noam Shazeer, Niki Parmar, Jakob Uszkoreit, Llion Jones, Aidan N Gomez, Łukasz Kaiser, and Illia Polosukhin. Attention is all you need. In *Advances in neural information processing systems*, pages 5998–6008, 2017.
- [53] Xiyuan Wang and Muhan Zhang. How powerful are spectral graph neural networks, 2022. URL <https://arxiv.org/abs/2205.11172>.
- [54] Floris Geerts. The expressive power of kth-order invariant graph networks. *ArXiv*, abs/2007.12035, 2020.
- [55] Thang Luong, Hieu Pham, and Christopher D. Manning. Effective approaches to attention-based neural machine translation. In *Proceedings of the 2015 Conference on Empirical Methods in Natural Language Processing*, pages 1412–1421, Lisbon, Portugal, September 2015. Association for Computational Linguistics. doi: 10.18653/v1/D15-1166. URL <https://aclanthology.org/D15-1166>.
- [56] Keyulu Xu, Chengtao Li, Yonglong Tian, Tomohiro Sonobe, Ken-ichi Kawarabayashi, and Stefanie Jegelka. Representation learning on graphs with jumping knowledge networks. *CoRR*, abs/1806.03536, 2018. URL <http://arxiv.org/abs/1806.03536>.
- [57] Linyuan Lü and Tao Zhou. Link prediction in complex networks: A survey. *Physica A: Statistical Mechanics and its Applications*, 390(6):1150–1170, 2011.

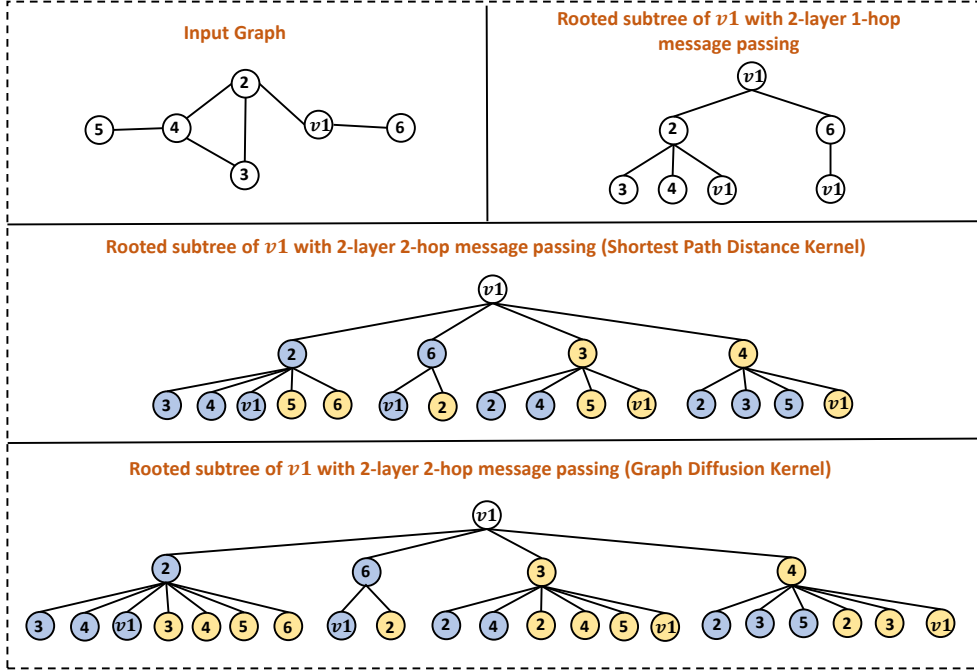


Figure 2: The rooted subtree of node v_1 with 1-hop message passing and K -hop message passing. Here we assume that $K = 2$ and the number of layers is 2.

A More about the K -hop kernel and K -hop message passing

In this section, we further discuss two different types of K -hop kernels and the K -hop message passing.

A.1 More about K -hop kernel

First, recall the shortest path distance and graph diffusion kernel in Definition 1 and 2. Given two definitions, the first thing we can conclude is that the K -hop neighbors of node v under two different kernels will be the same, namely $\mathcal{N}_{v,G}^{K,spd} = \mathcal{N}_{v,G}^{K,gd}$ as both two kernels capture all nodes that can be reached from node v within the length of K . Second, we have $\mathcal{N}_{v,G}^{1,spd} = Q_{v,G}^{1,spd} = \mathcal{N}_{v,G}^{1,gd} = Q_{v,G}^{1,gd}$, which means the neighbor set is same for both shortest path distance kernel and graph diffusion kernel when $K = 1$. The third thing is that $Q_{v,G}^{k,spd}$ will not always equal to $Q_{v,G}^{k,gd}$ for some k . Since for shortest path distance kernel, one node will only appear in one of $Q_{v,G}^{k,spd}$ for $k = 1, 2, \dots, K$. Instead, nodes can appear in multiple $Q_{v,G}^{k,gd}$. This is the key reason why the choice of the kernel can affect the representation power of K -hop message passing.

A.2 More about K -hop message passing

Here, we use an example shown in Figure 2 to illustrate how the K -hop message passing works and compare it with the 1-hop message passing. The input graph is shown on the left top of figure. Suppose we want to learn the representation of node v_1 using 2 layer message passing GNNs. First, if we perform 1-hop message passing, it will encode a 2-height rooted subtree, which is shown on the right top of figure. Note that each node is learned using the same set of parameters, which is indicated by filling each node with the same color (white in the figure). Now, we consider performing 2-hop message passing with the shortest path distance kernel. The rooted subtree of node v_1 is shown in the middle of the figure. we can see that at each height, both 1-th hop neighbors and 2-th hop neighbors are included. Furthermore, different sets of parameters are used in different hops, which is indicated by filling nodes in the different hops with different colors (blue for 1-th hop and yellow for 2-th hop). Finally, at the bottom of the figure, we show the 2-hop message passing graph neural network with

graph diffusion kernel. It is easy to see the rooted subtree is different from the one that uses the shortest path distance kernel, as nodes can appear in both 1-th hop and 2-th hop of neighbors.

B Discussion on existing K -hop message passing GNNs

In this section, we briefly characterize and discuss several existing K -hop GNN models.

B.1 Shortest path distance kernel

GINE+ [15]: GINE+ tries to increase the representation power of graph convolution by increasing the kernel size of convolution. However, in l layer of GINE+, it only aggregates information from the neighbor of hop 1, 2, ..., l , which means that after L layer of convolution, the GINE+ still has a receptive field of size L . By simultaneously considering information from multi-hop neighbors with the shortest path distance kernel, the expressive power of a L layer of K -hop GNN described in the main paper is at least no worse than a L layer GINE+.

Graphormer [20]: Graphormer introduce a new way to apply transformer architecture [52] on graph data. In each layer of Graphormer, the shortest path distance is used as spatial encoding to adjust the attention score between each node pair. Although the Graphormer does not apply the K -hop message passing directly, the attention mechanism (each node can see all the nodes) with the shortest path distance feature implicitly encodes a rooted subtree similar to the K -hop message passing with the shortest path distance kernel. To see it clearly, suppose we have K -hop message passing with $K = \infty$ and graphs only have one connected component. It will aggregate all the nodes at each layer, which is similar to Graphormer. Meanwhile, the injective message and update function implicitly encode the shortest path distance to each node in aggregation. Then it is trivial to see that Graphormer is actually a special case of K -hop message passing with the shortest path distance kernel.

B.2 Spectral-based GNNs and graph diffusion kernel

Spectral GNNs: spectral-based GNNs serve as an important type of graph neural network and gain lots of interest in recent years. Here we only consider one layer as spectral-based GNNs usually only use 1 layer. the general spectral GNNs can be written as:

$$Z = \phi \left(\sum_{k=0}^K \alpha_k \rho(\hat{L}^k) \varphi(x) \right) \quad (6)$$

Where ϕ and φ are typically multi-layer perceptrons (MLPs), \hat{L} is normalized laplacian matrix, ρ is an element-wise function of matrix. In normal spectral GNNs, ρ is always an identity mapping function. We can see spectral GNNs have a close relationship to K -hop message passing with graph diffusion kernel as \hat{L}^k actually compute the $Q_{v,G}^{k,gd}$ for each node by only keeping element in the matrix that is larger than 0. As K in Equation (6) can be greater than 1, it looks like spectral GNNs fit Proposition 1 as well. However, according to Proposition 4.3 in [53], all such spectral-based methods have expressive power no more than 1-WL test. This seems like a discrepancy. The reason lies in the ρ function in Equation (6). K -hop message passing with graph diffusion kernel can be regarded as using a non-linear ρ function shown in the following:

$$\rho(x) = \begin{cases} 1 & x > 0 \\ 0 & \text{others} \end{cases} \quad (7)$$

This non-linear function is the key difference between the normal spectral GNNs and K -hop message passing. This non-linear function endows normal spectral GNNs with expressive power greater than 1-WL test.

MixHop [11], **GPR-GNN** [14], and **MAGNA** [13]: All three methods extend the scope of 1-hop message passing by consider multiple graph diffusion step simultaneously. However, for all these methods, they use normal spectral GNNs as the base encoder and thus they follow Proposition 4.3 in [53] instead of Proposition 1. It can be seen as a "weak" version of K -hop message passing with graph diffusion kernel.

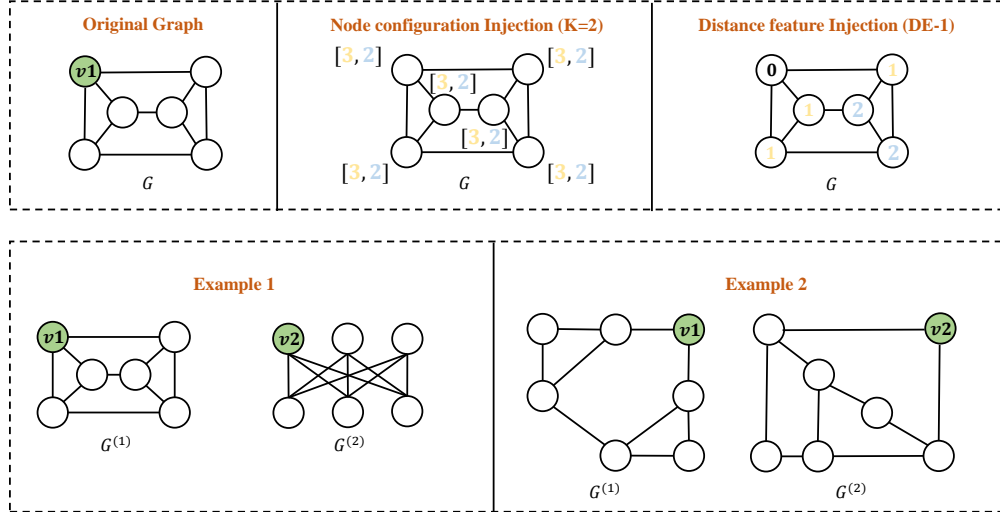


Figure 3: The upper part: graph with node configuration as the injected label and DE-1 as the injected label on the center node. The bottom part: two pairs of non-isomorphic graphs where the node pair in example 1 can be distinguished by DE-1 and the node pair in example 2 can be distinguished by K -hop message passing.

C Comparison between K -hop message passing and Distance Encoding

In this section, we further discuss the connection and difference between K -hop message passing and Distance Encoding [21]. Here we assume that the kernel of K -hop message passing is the shortest path distance and Distance Encoding with the shortest path distance as distance feature.

To simplify the discussion, suppose there are two graphs $G^{(1)} = (V^{(1)}, E^{(1)})$ and $G^{(2)} = (V^{(2)}, E^{(2)})$. We pick two nodes v_1 and v_2 from each graph respectively and learn the representation for these two nodes. First, let us consider what 1 layer K -hop message passing and DE-1 without message passing. As we stated in the main paper, 1 layer of K -hop message passing actually injects each node with the label of node configuration. Instead, DE-1 injects each node with the distance to the center node (v_1 and v_2 here). Then we can see there is a clear difference between the two methods even if they all implicitly or explicitly use the distance feature as shown in the upper part of Figure 3. Next, it is easy to see that applying $L + 1$ layer K -hop message passing is equivalent to applying L layer K -hop message passing on a graph with node configuration as the initial label. Applying L layer DE-1 is equivalent to applying L layer 1-hop message passing on a graph with the distance to the center node as the initial label. In the following, we show that the two methods cannot cover each other in terms of distinguishing nodes:

Proposition 2. *For two non-isomorphic graphs $G^{(1)} = (V^{(1)}, E^{(1)})$ and $G^{(2)} = (V^{(2)}, E^{(2)})$, we pick two nodes v_1 and v_2 from each graph respectively. Then there exist pairs of graphs that nodes v_1 and v_2 can be distinguished by K -hop message passing with the shortest path distance kernel but not DE-1, and vice versa.*

To prove the proposition, we provide two examples in the lower part of Figure 3. Example 1 in the figure is exactly the same pair of regular graphs in example 1 of Figure 1. As discussed before, K -hop message passing with the shortest path distance kernel cannot distinguish node v_1 and v_2 . However, after injecting the distance feature to the center node in two graphs and performing 2 layers of message passing, DE-1 is able to assign different representations for two nodes. In example 2, DE-1 cannot distinguish nodes v_1 and v_2 in the two graphs, even if they are not regular graphs. Instead, using K -hop message passing with only $K = 2$, the two nodes will get different representations. We omit the detailed procedure here as it is easy to validate. Using these two examples, we have shown that K -hop message passing and DE-1 are not equivalent to each other even if they all use the shortest path distance feature. The root reason is that although DE-1 uses the distance feature, it still aggregates information only from 1-hop neighbors in each iteration, while K -hop message passing directly aggregates information from all K -hop neighbors. That is, their ways of using distance information are different. However, we also notice that in example 2, if we label the graph with DE-1 on another pair of nodes, two nodes can be distinguished, which means DE-1 is able to distinguish these two graphs. **However, to achieve that, DE-1 need to label the graph n times and run the**

message passing on all n labeled graphs. Instead, K -hop message passing only needs to run the message passing once, which is both space and time efficiency.

Besides DE-1, Li et al. [21] also proposed the DEA-GNN which is at least no less powerful than DE-1. The DEA-GNN extends DE-1 by simultaneously aggregating all other nodes in the graph but the message is encoded with the distance to the center node. This can be seen as exactly performing K -hop message passing. In other words, DEA-GNN is the combination of K -hop message passing and DE-1. Therefore it is easy to see:

Proposition 3. *The DEA-GNN [21] is at least equally powerful as K -hop message passing with the shortest path distance kernel.*

D Proof of Theorem 1

In this section, we prove the Theorem 1. Our proof is inspired by the recent results in SUN [22], which bound all subgraph-based GNN with 3-WL test by proving that all such methods can be implemented by 3-IGN. Here we prove that K -hop message passing can also be implemented by 3-IGN. We will not discuss the detail of 3-IGN and all its operations. Instead, we directly follow all the definitions and notations and refer to reader Appendix B of [22] for more details.

K -hop neighbor extraction: To implement the K -hop message passing, we first implement the extraction of K -hop neighbors. The key insight is that we can use the l -th channel in X_{ii} to store whether node j is the neighbor of node i at l -th hop, which is similar to the extraction of ego-network. Here we suppose $d \geq K$. Same as all node selection policies, we first lifting the adjacency A to a three-way tensor $\mathcal{Y} \in \mathbb{R}^{n^3 \times d}$ using broadcasting operations:

$$X_{ii}^{(0)} = \beta_{i,i,i} A_{ii} \quad (8)$$

$$X_{ji}^{(0)} = \beta_{*,i,i} A_{ii} \quad (9)$$

$$X_{ij}^{(0)} = \beta_{i,i,j} A_{ij} \quad (10)$$

$$X_{ji}^{(0)} = \beta_{i,j,i} A_{ij} \quad (11)$$

$$X_{kij}^{(0)} = \beta_{*,i,j} A_{ij} \quad (12)$$

Now, $X_{ij}^{(0),1}$ store the 1-hop neighbors of node i . Next, l -th hop neighbor of node i is computed and stored in $X_{ij}^{(0),l}$. To get neighbor of l -th hop for $l = 2, 3, \dots, K$, we first copy it into $d + 1$ channels:

$$X_{ijj}^{(1)} = \kappa_{:d/(d+1)}^{:d} X_{ijj}^{(0)} + \kappa_{d+1:d+1}^{:l} \beta_{i,j,j} X_{ijj}^{(0)} \quad (13)$$

The $d + 1$ -th channel is used for compute high-order neighbors. Next, we extract all K hop neighbors by iteratively following steps $K - 1$ times and describe the generic l -th step. We first broadcast the current reachability pattern into X_{ijk} , writing it into the l -th channel:

$$X_{ijk}^{(l,1)} = X_{ijk}^{(l-1)} + \kappa_{l:l}^{d+1:d+1} \beta_{i,*,j} X_{ijj}^{(l-1)} \quad (14)$$

Then, a logical AND is performed to get the new reachability. Then write back the results into the l -th channel:

$$X_{ijk}^{(l,2)} = \varphi_{l:l/(d+1)}^{(\wedge),l} X_{ijk}^{(l,1)} \quad (15)$$

Next, we get all nodes that can be reached within l hops by performing pooling, clipping, and copy back to $d + 1$ channel:

$$X_{ijj}^{(l,3)} = \kappa_{:d/(d+1)}^{:d} X_{ijj}^{(l,2)} + \kappa_{d+1:l}^{:l} \beta_{i,j,j} \pi_{i,j} X_{ijk}^{(l,2)} \quad (16)$$

$$X_{ijj}^{(l,4)} = \left[\kappa_{:d/(d+1)}^{:d} \quad \varphi_{d+1:d+1}^{(\downarrow)d+1:d+1} \right] X_{ijj}^{(l,3)} \quad (17)$$

Now $X_{ijj}^{(l,4),d+1}$ save all the nodes that can be reached at l -th hop. Finally, we extract the l -th hop neighbor and copy it into l -th channel. For graph diffusion kernel, current result is itself neighbors for graph diffusion kernel, which mean we only need to copy it:

$$X_{ij}^{(l)} = X_{ijj}^{(l,4)} + \kappa_{l:l}^{d+1:d+1} \beta_{i,i,j} X_{ijj}^{(l,4)} \quad (18)$$

For shortest path distance kernel, we need to nullify all the nodes that already existed in the previous hops. To achieve, we need to first compute is a node exist in previous hop and then nullify it:

$$X_{ijj}^{(l,5)} = X_{ijj}^{(l,4)} + \kappa_{l:l}^{d+1:d+1} \beta_{i,*,j} X_{ijj}^{(l,4)} \quad (19)$$

$$X_{ijj}^{(l,6)} = \sum_{i=1}^{l-1} \kappa_{d+1:d+1}^{i:i} X_{ijj}^{(l,5)} \quad (20)$$

$$X_{ijj}^{(l)} = X_{ijj}^{(l,4)} + \varphi_{l:l}^{(\wedge)l,d+1} \varphi_{d+1}^{(l)d+1} X_{ijj}^{(l,6)} \quad (21)$$

Where $\varphi_b^{(l)a}$ is logical not function that output 0 if input is not 0 and vice versa for channel a and write result into channel b . Here we omit the detail implementation as it is easy to implement using ReLu function. Finally, we bring all other orbits tensors to the original dimensions:

$$X_{iii} = \kappa_{:d}^{:d} X_{iii}^{(l)} \quad (22)$$

$$X_{ijj} = \kappa_{:d}^{:d} X_{ijj}^{(l)} \quad (23)$$

$$X_{iij} = \kappa_{:d}^{:d} X_{iij}^{(l)} \quad (24)$$

$$X_{iji} = \kappa_{:d}^{:d} X_{iji}^{(l)} \quad (25)$$

$$X_{ijk} = \kappa_{:1/(d)}^{:1} X_{ijk}^{(l)} \quad (26)$$

Now, we have successfully implement K -hop neighbor extraction algorithm using 3-IGN.

K -hop message passing: To implement the message and update function for each layer, we use same base encoder as [17]. Other type of base encoders and combine function can be implemented by similar way. We follow the same procedure of implementing base encoder of DSS-GNN as stated in [22]. Note here for each hop the procedure is similar therefore we state the generic l -th hop. The key insight is that, in K -hop message passing, we are actually not working on each subgraph but the original graph, which means all the operation can be implemented in the orbit tensor X_{iii} and X_{iij} .

Message broadcasting: This procedure is similar to the base encoder of DSS-GNN but here we only need to broadcast X_{iij} . However, since we need to perform message passing for K times, we need to broadcast it K times:

$$X_{iij}^{(t,1)} = \kappa_{:d/((K+1)d)}^{:d} X_{iij}^{(t)} + \sum_{i=1}^K \kappa_{id+1:(i+1)d/(K+1)d}^{:i} \beta_{iij} X_{iij}^{(t)} \quad (27)$$

Message sparsification and aggregation: Similar to DSS-GNN, here we need to nullify the message that from nodes which are not l -th hop neighbors. Here we define the following function:

$$f_{ij}^{\odot} \left(X_{aab}^{(t,1)} \right)_l = \begin{cases} \mathbf{0}_d & \text{if } X_{aab}^{(t,1),l} = 0 \\ X_{aab}^{(t,1),l(d+1):(l+1)d} & \text{otherwise} \end{cases} \quad (28)$$

The function is used to nullify message for l -th hop. It is easy to valid the existing of such function follow the same procedure in [22] therefore we omit the detail. Next, the message sparsification can be implemented by:

$$X_{ij}^{(t,3)} = \left[\kappa_{:d}^{:d} \quad \varphi_1^{(\odot_{ijj})} \quad \dots \quad \varphi_K^{(\odot_{ijj})} \right] X_{ij}^{(t,2)} \quad (29)$$

Then, the message function for K -hop message passing is:

$$X_{iii}^{(t,4)} = \kappa_{:d}^{:d} X_{iii}^{(t,3)} + \kappa_{d+1}^{d+1} \beta_{iii} \pi_i X_{ijj}^{(t,3)} \quad (30)$$

Update Then, the update function is implemented using linear transformation. In K -hop message passing, each hop need independent parameter set. Here in order to operate on constructed tensor, we define $W_t^l = [W_{t,1}^l || W_{t,2}^l || \dots || W_{t,K}^l]$, where $W_{t,i}^l = \mathbf{0}_d$ if $i \neq l$. Then, the update function is:

$$X_{iii}^{(t,5)} = \sum_{l=1}^K \sigma \left(W_t^l X_{iii}^{(t,4)} \right) \quad (31)$$

Combine: Finally, we implement sum combine function. The combine function is can be implemented by a simple MLP:

$$X_{iii}^{(t+1)} = \varphi_d^f \left(X_{iii}^{(t,4)} \right) \quad (32)$$

$$X_{jii}^{(t+1)} = \beta_{jii} X_{iii}^{t+1} \quad (33)$$

Now, we successfully implement both K -hop neighbor extraction and K -hop message passing layer. Note that other parts like readout function can be easy implemented and we omit the detail. This means the expressive power of K -hop message passing with either graph diffusion kernel or shortest path distance kernel is bounded by 3-IGN. Based on the Theorem 2 in [54], we conclude the Theorem 1.

However, we also notice that across all proof, the only operation that need to be done in 3-order tensor but not 2-order tensor are Equation (14) and Equation (15). All other operations can be implemented by 2-order tensor.

E Proof of Theorem 2

In this section, we prove the Theorem 2. The proof is based on NGNN [25] and Distance Encoding [21]. Suppose there are two n -node r -regular graphs $G^{(1)} = (V^{(1)}, E^{(1)})$ and $G^{(2)} = (V^{(2)}, E^{(2)})$. We pick two nodes v_1 and v_2 from each graph respectively. Assume here we use the shortest path distance kernel and the KP-GNN can only encode the information of peripheral edges, which means that the model can only distinguish two nodes if they have a different number of peripheral edges at some hops (assume no edge feature). Before we start the proof, we first introduce *cross edge configuration*:

Definition 6. *The cross edge configuration between $Q_{v,G}^{k,spd}$ and $Q_{v,G}^{k+1,spd}$ is a list $C_{v,G}^{k,spd} = (c_{v,G}^{1,k}, c_{v,G}^{2,k}, \dots)$ where $c_{v,G}^{i,k}$ denotes the number of nodes in $Q_{v,G}^{k+1,spd}$ of which each has exactly i edges from $Q_{v,G}^{k,spd}$.*

Note that if $C_{v_1, G^{(1)}}^{k, spd} = C_{v_2, G^{(2)}}^{k, spd}$, we have $|Q_{v_1, G^{(1)}}^{k+1, spd}| = |Q_{v_2, G^{(2)}}^{k+1, spd}|$. However, the statement is not always true if reversed. Namely, even if $|Q_{v_1, G^{(1)}}^{k+1, spd}| = |Q_{v_2, G^{(2)}}^{k+1, spd}|$, we cannot argue that $C_{v_1, G^{(1)}}^{k, t} = C_{v_2, G^{(2)}}^{k, t}$. Next, we introduce Lemma 1 from Distance encoding [21]:

Lemma 1. *For two graphs $G^{(1)} = (V^{(1)}, E^{(1)})$ and $G^{(2)} = (V^{(2)}, E^{(2)})$ that are uniformly independently sampled from all n -node r -regular graphs, where $3 \leq r < \sqrt{2 \log n}$, we pick two nodes v_1 and v_2 from two graphs respectively. Then there is at least one $i \in [\frac{1}{2} \frac{\log n}{\log(r-1-\epsilon)}, (\frac{1}{2} + \epsilon) \frac{\log n}{\log(r-1-\epsilon)}]$ with probability $1 - o(n^{-1})$ such that $C_{v_1, G^{(1)}}^{i, spd} \neq C_{v_2, G^{(2)}}^{i, spd}$. Moreover, with at least the same probability, for all $i \in [\frac{1}{2} \frac{\log n}{\log(r-1-\epsilon)}, (\frac{2}{3} - \epsilon) \frac{\log n}{\log(r-1-\epsilon)}]$, the number of edges between $Q_{v_j, G^{(j)}}^{i, spd}$ and $Q_{v_j, G^{(j)}}^{i+1, spd}$ are at least $(r-1-\epsilon)|Q_{v_j, G^{(j)}}^{i, spd}|$ for $j \in \{1, 2\}$.*

The proof can be found by following steps 1-3 in the proof of Theorem 3.3 in [21].

Now we set the $K = \lceil (\frac{1}{2} + \epsilon) \frac{\log n}{\log(r-1-\epsilon)} \rceil$ and using KP-GNN with only 1 layer. From the Lemma 1, we know that with probability $1 - o(n^{-1})$, there exist at least one $k < K$ with $C_{v_1, G^{(1)}}^{k, spd} \neq C_{v_2, G^{(2)}}^{k, spd}$. We select the smallest k and start our proof.

1. If $A_{v_1, G^{(1)}}^{k, spd} \neq A_{v_2, G^{(2)}}^{k, spd}$, then we already prove it by proposition 1. Therefore, the condition we need to prove is that when $A_{v_1, G^{(1)}}^{k, spd} = A_{v_2, G^{(2)}}^{k, spd}$, which means $|Q_{v_1, G^{(1)}}^{k, spd}| = |Q_{v_2, G^{(2)}}^{k, spd}|$ for each $k = 1, 2, \dots, K$.
2. Next, we know that the summation of all elements in $C_{v_j, G^{(j)}}^{k, spd}$ is equal to $|Q_{v_j, G^{(j)}}^{k+1, spd}|$ for $j \in \{1, 2\}$. As we know that $|Q_{v_1, G^{(1)}}^{k+1, spd}| = |Q_{v_2, G^{(2)}}^{k+1, spd}|$ based on above point, $C_{v_1, G^{(1)}}^{k, spd} \neq C_{v_2, G^{(2)}}^{k, spd}$ means that the number of edge that link from nodes in $Q_{v_1, G^{(1)}}^{k, spd}$ to nodes in $Q_{v_1, G^{(1)}}^{k+1, spd}$ is not equal to that of v_2 .
3. Meanwhile, since we are studying the regular graph, each node has the same degree. It means that the number of edge links to a given node is the same for both graph $G^{(1)}$ and $G^{(2)}$ (the node degree r).
4. The edges of node in $Q_{v_1, G^{(1)}}^{k, spd}$ must connect to nodes in either $Q_{v_1, G^{(1)}}^{k-1, spd}$, $Q_{v_1, G^{(1)}}^{k, spd}$, or $Q_{v_1, G^{(1)}}^{k+1, spd}$. This statement also holds for $G^{(2)}$. Since we have $C_{v_1, G^{(1)}}^{k-1, spd} = C_{v_2, G^{(2)}}^{k-1, spd}$ given the assumption that k is the smallest value to induce different cross edge configuration, we know that the number of edge link from $Q_{v_1, G^{(1)}}^{k, spd}$ to $Q_{v_1, G^{(1)}}^{k-1, spd}$ must equal to the number of edge link from $Q_{v_2, G^{(2)}}^{k, spd}$ to $Q_{v_2, G^{(2)}}^{k-1, spd}$.
5. Combine point 3 and 4, we conclude that the number of edge link from $Q_{v_1, G^{(1)}}^{k, spd}$ to $Q_{v_1, G^{(1)}}^{k, spd}$ is not equal to that of v_2 , namely $|E(Q_{v_1, G^{(1)}}^{k, spd})| \neq |E(Q_{v_2, G^{(2)}}^{k, spd})|$.

The above statement proved that in two r -regular graphs, $|E(Q_{v_1, G^{(1)}}^{k, spd})| \neq |E(Q_{v_2, G^{(2)}}^{k, spd})|$ if $C_{v_1, G^{(1)}}^{k, spd} \neq C_{v_2, G^{(2)}}^{k, spd}$. Meanwhile, it is easy to see that as long as $|E(Q_{v_1, G^{(1)}}^{k, t})| \neq |E(Q_{v_2, G^{(2)}}^{k, t})|$ for some k , a KP-GNN with $K > k$ and only 1 layer can produce different representation for node v_1 and v_2 . Combine both statements, we conclude that a KP-GNN with only peripheral edge information can produce different representation for node v_1 and node v_2 in graph $G^{(1)}$ and $G^{(2)}$.

F Proof of Theorem 3 and more discussion on distance regular graph and subgraph based GNNs

F.1 Proof of Theorem 3

To prove Theorem 3, we first give the definition of *distance regular graph*.

Definition 7. A distance regular graph is a regular graph such that for any two nodes v and u , the number of nodes with the distance of i from v and distance of j from u depends only on i , j and the distance between v and u .

Furthermore, we only consider the connected distance regular graphs with no multi-edge or self-loop. Such graphs can be characterized by *intersection array*.

Definition 8. The intersection array of a distance regular graph with diameter d is an array of integers $(b_0, b_1, \dots, b_{d-1}; c_1, c_2, \dots, c_d)$, where for all $1 \leq j \leq d$, b_j gives the number of neighbors of u with distance $j + 1$ from v and c_j gives the number of neighbors of u with distance $j - 1$ from v for any pair of (v, u) in graph with distance j .

Given the definition of distance regular graph and intersection array, we can propose the first lemma.

Lemma 2. Given a distance regular graph G with intersection array $(b_0, b_1, \dots, b_{d-1}; c_1, c_2, \dots, c_d)$. Pick a node v from G , the peripheral subgraph $G_{v,G}^{j,spd}$ is a n -sized r -regular graph with $n = |Q_{v,G}^{j,spd}|$ and $r = b_0 - b_j - c_j$

Proof. Given a distance regular graph G with intersection array $(b_0, b_1, \dots, b_{d-1}; c_1, c_2, \dots, c_d)$, from the definition of intersection array, for node v in G , $Q_{v,G}^{j,spd}$ is the node set that have distance j from node v . Then, b_j is the number of neighbors for each node in $Q_{v,G}^{j,spd}$ that have distance $j + 1$ to node v . It is easy to see that these neighbors must belong to $Q_{v,G}^{j+1,spd}$, which means that b_j is also the number of edge for a node in $Q_{v,G}^{j,spd}$ that connect to nodes in $Q_{v,G}^{j+1,spd}$. Similarly, c_j is the number of edge for a node in $Q_{v,G}^{j,spd}$ that connect to nodes in $Q_{v,G}^{j-1,spd}$. For node $u \in Q_{v,G}^{j,spd}$, we know that the edges of u must connect to either $Q_{v,G}^{j+1,spd}$, $Q_{v,G}^{j,spd}$, or $Q_{v,G}^{j-1,spd}$. Since the degree of node u is b_0 , then the number of edge that connect node u to nodes in $Q_{v,G}^{j,spd}$ is $b_0 - b_j - c_j$. The above statement holds for each $u \in Q_{v,G}^{j,spd}$, which means all nodes $u \in Q_{v,G}^{j,spd}$ have same node degree. Meanwhile, the node set of peripheral subgraph $G_{v,G}^{j,spd}$ is exactly $Q_{v,G}^{j,spd}$. Combine two statements, we can conclude that $G_{v,G}^{j,spd}$ is a n -sized r -regular graph with $n = |Q_{v,G}^{j,spd}|$ and $r = b_0 - b_j - c_j$. \square

Given the Lemma 2, we know that the peripheral subgraph of a node in any distance regular graph is itself a regular graph. Next, given two non-isomorphic distance regular graphs $G^{(1)}$ and $G^{(2)}$ with the same intersection array, there are total d pairs of regular peripheral subgraphs. If the KP-GNN can distinguish two regular graphs at some hop $j \leq d$, then the KP-GNN can distinguish v_1 and v_2 in graph $G^{(1)}$ and $G^{(2)}$. Finally, the following lemma describes when can KP-GNN achieve it.

Lemma 3. Given a KP-GNN with message function implemented as Equation 5, it can distinguish two non-isomorphic n -sized r regular graphs if $r = 2$.

Proof. It is straightforward to see that KP-GNN can count the number of components and the number of edges in each component. Given two non-isomorphic n -sized 2-regular graphs, each node has two edges, therefore, such regular graphs must be a set of circles. since two graphs have the same number of edges, then, if two graphs are non-isomorphic, the number of circles must be different for two graphs. Therefore, by counting the number of circles, the KP-GNN can distinguish two graphs. \square

Now, we can conclude that KP-GNN implemented as Equation 5 can distinguish two non-isomorphic distance regular graphs with the same intersection array, whenever there exist some $j \leq d$ with $b_0 - b_j - c_j = 2$ by distinguishing two peripheral subgraphs at j . Notes that for $r = 1$ and $r = 0$, there is no non-isomorphic structure and KP-GNN cannot generate a different representation.

F.2 More discussion on distance regular graphs

Distance Encoding has limited power on distinguishing distance regular graph according to Theorem 3.7 in [21]. Basically, Distance Encoding with the shortest path distance cannot distinguish any two connected distance regular graphs with the same intersection arrays. Instead, as we discussed above, the KP-GNN has the ability to distinguish some distance regular graphs. To further illustrate it, we leverage another example in Figure 4. The Figure 4 displays two distance regular graph

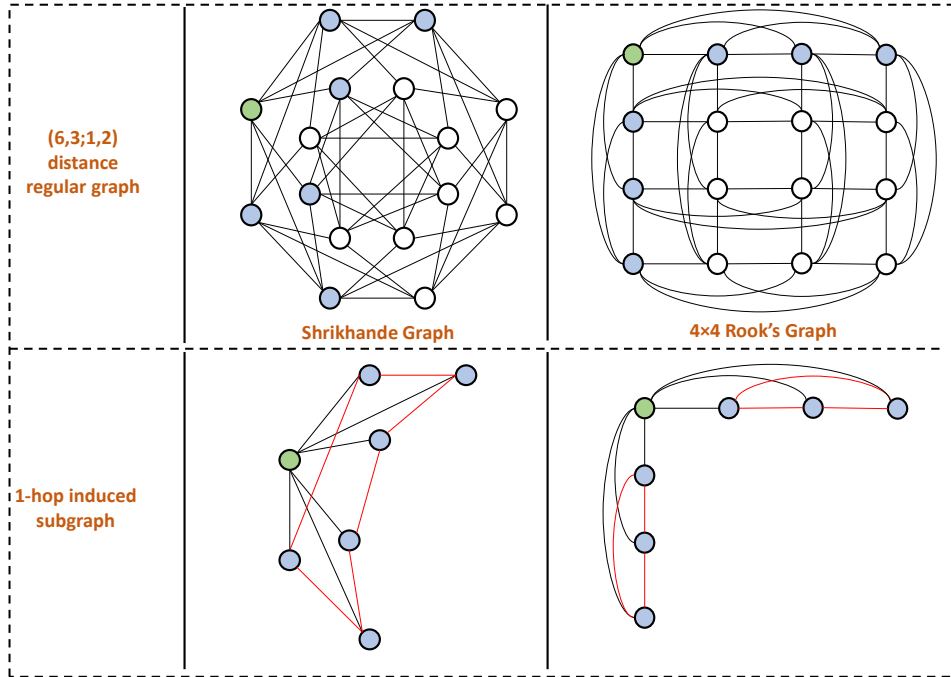


Figure 4: An example of two non-isomorphic distance regular graph with intersection array $(6, 3; 1, 2)$

with intersection array of $(6, 3; 1, 2)$. The left one is Shrikhande graph and the right one is 4×4 Rook's graph. The distance encoding cannot distinguish the green node in two graphs as they belong to distance regular graphs with the same intersection array. Now, let's look at the 1-hop induced subgraph of the green node. In Shrikhande graph, there are 6 peripheral edges, which are marked with red. Further, 6 edges constitute a circle. In the 4×4 Rook's graph, there are still 6 peripheral edges. However, 6 edges constitute two circles with 3 edges in each circle, which is different from the Shrikhande graph. Then, by counting the number of components and edges in each component, KP-GNN is able to distinguish two green nodes by assigning different representations.

F.3 Discussion on subgraph-based GNNs

Both the subgraph-based GNNs like NGNN [25], GNNAK [26], ESAN [28], and KP-GNN leverage the information in the subgraph to enhance the power of message passing. In this section, we discuss the difference between two frameworks. Our discussion focus on subgraph-based GNNs that utilize ego-network for each node to generate subgraphs. Firstly, in KP-GNN, the message passing is performed on the whole graph instead of the subgraphs. This means that for each node, there is only one representation to be learned. Instead, for subgraph-based GNNs, the message passing is performed separately for each subgraph and each node could have multiple representations depending on which subgraph it is in. Secondly, in subgraph-based GNNs, they consider the subgraph as a whole without distinguishing nodes at different hops. Instead, KP-GNN takes one step further by dividing the subgraph into two parts. The first part is the hierarchy of neighbors at each hop. The second part is the connection structure between nodes in each hop. This gives us a better point of view to design a more powerful learning method.

From the Corollary 7 in [22], we know that all subgraph-based GNNs with node selection as subgraph policy is bounded by 3-WL, which means they cannot distinguish any distance regular graph. **This conclusion confirms the higher power of KP-GNN in terms of distinguishing distance regular graphs, even if all methods leverage subgraph information for better expressive power.** However, it is currently unknown whether the KP-GNN is strictly more powerful than subgraph-based GNNs, we leave it to future works.

G Time, space complexity and limitation of K -hop message passing and KP-GNN

G.1 Time and space complexity

In this section, we analyze the time and space complexity. To simplify the analysis, we first consider the shortest path distance kernel, as graph diffusion kernel has both time and space complexity no less than the shortest path distance kernel. Denote graph G with n node and m edges.

Space complexity: For both K -hop message passing and KP-GNN, as we only need to maintain one representation for each node, the space complexity is $O(n)$ like in vanilla 1-hop message passing.

Time complexity: First, we analyze the time complexity of K -hop message passing GNNs. For each node, suppose in the worst case we extract neighbors from all nodes from all hops, the number of neighbors we need to aggregate from all hops is n (all nodes in the graph). Then, n nodes need at most $O(n^2)$ time complexity. Next we analyze the time complexity of KP-GNN. The additional time complexity comes from counting the connected components in the peripheral edges. Since each node has at most m peripheral edges (and the counting is linear to m), KP-GNN has a time complexity bounded by $O(n(n + m))$. However, since the counting can be done in a preprocessing step and reused at each message passing iteration, it will be amortized to zero finally. So the practical time complexity is still $O(n^2)$.

G.2 Discussion on the complexity

From the above analysis, we know that K -hop GNNs and KP-GNN only need $O(n)$ space complexity, which is equal to normal GNNs and much less than subgraph-based GNNs which require $O(n^2)$ space (due to maintaining a different representation for each node when appearing in different subgraphs). Thus, KP-GNN has a much better space complexity than subgraph-based GNNs, PPGN [23] (also $O(n^2)$) and 3-WL-GNNs ($O(n^3)$).

The worst-case time complexity of K -hop GNNs and KP-GNN is much higher than that of normal GNNs due to aggregating information from more than 1-hop nodes in each iteration. However, we also note that the larger receptive field could reduce the number of message passing iterations because 1-layer of K -hop message passing can cover the receptive field of K -layer 1-hop message passing. Furthermore, K -hop GNN and KP-GNN have better time complexity $O(n^2)$ than that of subgraph-based GNNs (which require $O(nm)$ for doing 1-hop message passing $O(m)$ in all n subgraphs). For sparse graphs, we can already save a factor of $d_{\text{avg}} = m/n$ complexity. For dense graphs, the worst-case time complexity of subgraph-based GNNs becomes $O(n \cdot n^2) = O(n^3)$, and our time complexity advantage becomes even more significant.

G.3 Limitations

We discuss the limitation of the proposed KP-GNN from two aspects.

Stability: Using K -hop instead of 1-hop can make the receptive field of a node increase with respect to K . For example, to compute the representation of a node with L layer K -hop, GNN, the node will get information from all LK -hop neighbors. The increased receptive field can hurt learning, as mentioned in GINE+ [15]. It is an intrinsic limitation that exists in all K -hop GNNs. GINE+ [15] proposed a new way to fix the receptive field as L by only considering $L - i$ layer representation of neighbor in i hop during the aggregation. We also apply this approach and it helps mitigate the issue and shows great practical performance gain.

Time complexity: As we show above, we need $O(n^2)$ time complexity for KP-GNN, which is much higher than $O(m)$ of MPNN. However, this limitation exists for all subgraph-based methods like NGNN [25], GNN-AK [26], and ESAN [28] as they all require $O(nm)$ time complexity [22]. This is the sacrifice for better expressive power.

H Implementation detail of KP-GNN

In this section, we discuss the implementation detail of KP-GNN. ¹

Combine function: 1-hop message passing GNNs do not have $COMBINE^l$ function. Here we introduce two different $COMBINE^l$ functions. The first one is the attention [55] based combination mechanism, which automatically learns the importance of representation for each node at each hop. The second one uses the well-known geometric distribution [13]. The weight of hop i is computed based on $\theta_i = \alpha(1 - \alpha)^i$, where $\alpha \in (0, 1]$. The final representation is calculated by weighted summation of the representation of all the hops.

Peripheral subgraph information: In the current implementation, KP-GNN only considers the number of components and the number of edges in each component in the peripheral subgraph. However, each node may have a different peripheral subgraph. To allow the model to work, we set thresholds for the maximum number of components and the maximum number of edges in each component in the implementation.

KP-GCN, KP-GIN, and KP-GraphSAGE: We implement KP-GCN, KP-GIN, and KP-GraphSAGE using the message and update function defined in GCN [1], GIN [7], and GraphSAGE [3] respectively. In each hop, independent parameter sets are used and the computation in each hop strictly follows the corresponding model. However, increasing the number of K will also increase the total number of parameters, which is not scalable to K . To avoid this issue, we design the K -hop message passing in the following way. Suppose the total hidden size of the model is H , then the hidden size of each hop is H/K . In this way, the model size is still in same scale even with large K .

KP-GIN+: In a normal K -hop message passing framework, all K -hop neighbors will be aggregated for each node. It means that, after L layers, the receptive field of GNN is LK . This may cause the unstable of the training as unrelated information may be aggregated. To alleviate this issue, we adapted the idea from GINE+ [15]. Specifically, we implement KP-GIN+, which apply exactly the same architecture of GINE+ except here we add peripheral subgraph information. At layer l , GINE+ only aggregates information from neighbors within l -hop, which makes a L layer GINE+ still have a receptive field of L . Note that in KP-GIN+, we use a shared parameter set for each hop.

Path encoding: To further utilize the information of graph structure on each hop, we introduce the path encoding to KP-GNN. Specifically, we not only count whether two nodes are neighbors at hop k , but also count the number of paths with length k between two nodes. Such information is easy to count as the A^k of a graph G with adjacency A is a path counter with length k . Then the information is added to the $AGG_k^{l,normal}$ function as additional features.

Other implementation: For all GNNs, we apply the Jumping Knowledge method [56] to get the final node representation. The possible methods include sum, mean, concatenation, last, and attention. Batch normalization is used after each layer.

I Experimental setting details

EXP: For the EXP dataset, we use KP-GIN+ with 4 layers and a hidden size of 60. The final node representation is output from the last layer and the pooling method is the summation. Through the experiment, we use 10-fold cross-validation. For each fold, we use 8 folds for training, 1 fold for validation, and 1 fold for testing. We select the model with the best validation accuracy and report the mean results across all folds. The training epoch is set to 40. In this experiment, we do not use path encoding. The learning rate is set to 0.001 and we use *ReduceLROnPlateau* learning rate scheduler with patience of 5 and a reduction factor of 0.5. The maximum number of the peripheral edge is 10 and we don't consider component information in EXP training.

Graph&Node property dataset: For graph and node property prediction tasks, we train models with independent 4 runs and report the mean results. The hidden size of models is set as 256. The final node representation is the concatenation of each layer. The pooling method is attention for graph property prediction tasks and sum for node property prediction tasks. The dropout rate is set as 0. The learning rate is 0.01 and we use *ReduceLROnPlateau* learning rate scheduler with patience of 10 and a reduction factor of 0.5. We use shortest path distance kernel. The maximum number of epochs

¹The implementation of KP-GNN can be found at <https://github.com/anoncodesub/KP-GNN>.

for each run is 250. The maximum number of the peripheral edge is 10 and the maximum number of the component is 5.

Graph substructure counting dataset: For graph substructure counting tasks, we train models with independent 4 runs and report the mean results. The hidden size of models is set as 256. The final node representation is the concatenation of each layer. The pooling method is summation. The dropout rate is set as 0. The learning rate is 0.01 and we use *ReduceLRonPlateau* learning rate scheduler with patience of 10 and a reduction factor of 0.5. We use the shortest path distance kernel. The maximum number of epochs for each run is 250. The maximum number of the peripheral edge is 10 and the maximum number of the component is 5.

TU datasets: For TU datasets, we use 10-fold cross-validation. We report result for both setting in [7] and [36]. For the first setting, we use 9 folds for training and 1 fold for testing in each fold. After training, we average the test accuracy across all the folds. Then a single epoch with the best mean accuracy and the standard deviation is reported. For the second setting, we still use 9 folds for training and 1 fold for testing in each fold but we directly report the mean best test results. For KP-GNN, we implement GCN [1], GraphSAGE [3] and GIN [7] version. we search (1)the number of layer {2, 3, 4}, (2)the number of hop {2, 3, 4}, (3) the kernel of K-hop {*spd, gd*}, and (4) the *COMBINE* function {*attention, geometric*}. The hidden size is 33 when $K = 3$ and 32 for the rest of the experiments. The final node representation is the concatenation of each layer and the pooling method is the summation. The dropout rate is set as 0.5, the number of training epochs for each fold is 350 and the batch size is 32. The initial learning rate is set as $1e - 3$ and decays with a factor of 0.5 after every 50 epochs.

QM9 dataset: For QM9 dataset, we implement KP-GIN+. The hidden size of the model is 128. The number of hops and the number of layers are both 8. The final node representation is the concatenation of each layer and the pooling method is attention. The dropout rate is 0. We use the shortest path distance kernel. The maximum number of the peripheral edge is 6 and the maximum number of the component is 3. We also use additional path encoding in each layer. The learning rate is 0.001 and we use *ReduceLRonPlateau* learning rate scheduler with patience of 5 and a reduction factor of 0.7. If the learning rate is less than 0.000001, the training is stopped.

OGB dataset: For ogbg-molhiv dataset, we run the experiment 10 times independently and report the mean results. For each run, the number of epochs is 60 and the batch size is 32. We implement the KP-GIN+ for the dataset. The hidden size is 64. The final node representation is the concatenation of each layer and the pooling method is the summation. We use the shortest path distance kernel. The number of hops and the number of layers are both 6. The initial learning rate is set as $1e - 3$ and decays with a factor of 0.5 after every 20 epochs. Moreover, the virtual node [16] and resistance distance [57] are introduced to further improve the model.

ZINC dataset: For ZINC dataset, we run the experiment 4 times independently and report the mean results. For each run, the maximum number of epochs is 500 and the batch size is 32. We implement the KP-GIN+ for the dataset. The hidden size is 136. The final node representation is the concatenation of each layer and the pooling method is the summation. We use the graph diffusion as kernel. The number of hops and the number of layers are both 8. The initial learning rate is 0.001 and we use *ReduceLRonPlateau* learning rate scheduler with patience of 10 and a reduction factor of 0.5. If the learning rate is less than 0.000001, the training is stopped.

J Datasets Description and Statistics

Table 8: Dataset statistics.

Dataset	#Tasks	# Graphs	Ave. # Nodes	Ave. # Edges
EXP	2	1200	44.4	110.2
Graph&Node property	3	5120/640/1280	19.5	101.1
Substructure counting	4	1500/1000/2500	18.8	62.6
MUTAG	2	188	17.93	19.79
D&D	2	1178	284.32	715.66
PTC-MR	2	344	14.29	14.69
PROTEINS	2	1113	39.06	72.82
IMDB-B	2	1000	19.77	96.53
QM9	12	129433	18.0	18.6
ZINC	1	10000 / 1000 / 1000	23.1	49.8
ogbg-molhiv	1	32901 / 4113 / 4113	25.5	54.1

K Proof of Injectiveness of Equation (3)

In this section, we formally prove that Equation (3) is an injective mapping of the neighbor representations at different hops. As here each layer l is doing exactly the same procedure, we only need to prove it for one iteration. Therefore we ignore the superscript and rewrite Equation (3) as:

$$\begin{aligned} m_v^k &= \text{MES}_k(\{(h_u, e_{uv}) | u \in Q_{v,G}^{k,t}\}), \quad h_v^k = \text{UPD}_k(m_v^k, h_v), \\ \hat{h}_v &= \text{COMBINE}(\{h_v^k | k = 1, 2, \dots, K\}) \end{aligned} \quad (34)$$

Next, we propose the following theorem:

Theorem 4. *There exists injective functions $\text{MES}_k, \text{UPD}_k, k = 1, 2, \dots, K$, and an injective multiset function COMBINE , such that \hat{h}_v is an injective mapping of $\{(k, \{(h_u, e_{uv}) | u \in Q_{v,G}^{k,t}\}, h_v) | k = 1, 2, \dots, K\}$.*

Proof. The existence of injective message passing ($\text{MES}_k, \text{UPD}_k$) and multiset pooling (COMBINE) functions are well proved in [7]. So below we prove the injectiveness of \hat{h}_v . First, we combine the MES_k and UPD_k together into ϕ_k :

$$h_v^k = \phi_k(\{(h_u, e_{uv}) | u \in Q_{v,G}^{k,t}\}, h_v). \quad (35)$$

Note that ϕ_k is still injective as the composition of injective functions is injective. Next, we need to prove that h_v^k is an injective mapping of $(k, \{(h_u, e_{uv}) | u \in Q_{v,G}^{k,t}\}, h_v)$. To prove it, we rewrite the function $\phi_k(\cdot)$ into $\phi(k)(\cdot)$, that is, ϕ is an injective function taking k as input and outputs a function $\phi_k = \phi(k)$. We let $\phi(k_1)(x_1)$ and $\phi(k_2)(x_2)$ output different values for $k_1 \neq k_2$ given any input x_1, x_2 , e.g., always let the final output dimension be k . Then, we can rewrite h_v^k as

$$\begin{aligned} h_v^k &= \phi(k)(\{(h_u, e_{uv}) | u \in Q_{v,G}^{k,t}\}, h_v) \\ &= \psi(k, \{(h_u, e_{uv}) | u \in Q_{v,G}^{k,t}\}, h_v) \end{aligned} \quad (36)$$

where we have composed the two injective functions $\phi(\cdot)$ and $\phi(k)(\cdot)$ into a single one $\psi(\cdot)$. Since given different k , $\phi(k)(\cdot)$ always outputs distinct values for any input, and given fixed k , $\phi(k)(\cdot)$ always outputs different values for different $(\{(h_u, e_{uv}) | u \in Q_{v,G}^{k,t}\}, h_v)$, the resulting

$\psi(\cdot)$ always outputs different values for different $(k, \{(h_u, e_{uv}) | u \in Q_{v,G}^{k,t}\}, h_v)$, i.e., it injectively maps $(k, \{(h_u, e_{uv}) | u \in Q_{v,G}^{k,t}\}, h_v)$. Thus, we have proved that h_v^k is an injective mapping of $(k, \{(h_u, e_{uv}) | u \in Q_{v,G}^{k,t}\}, h_v)$.

Finally, since COMBINE is an injective multiset function, we conclude that its output \hat{h}_v is an injective mapping of $\{(k, \{(h_u, e_{uv}) | u \in Q_{v,G}^{k,t}\}, h_v) \mid k = 1, 2, \dots, K\}$. \square